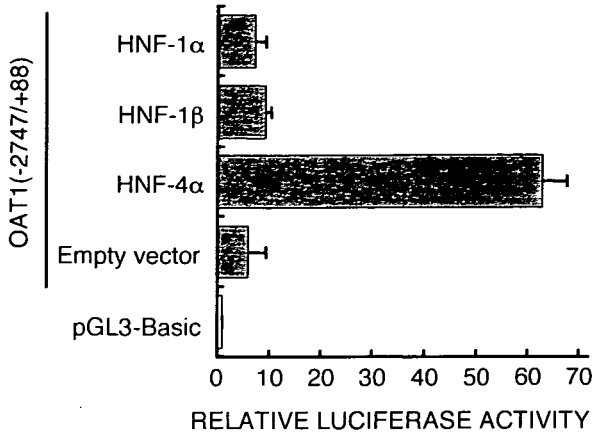

Fig. 2. Effects of hepatocyte nuclear factor (HNF)-1α, HNF-1β, and HNF-4α overexpression on human OAT1 promoter activity. OK cells were transiently transfected with 500 ng of a −2747/+88 construct and 500 ng of the expression vector for HNF-1α, HNF-1β, HNF-4α, or empty vector. Firefly luciferase activity was normalized to *Renilla* luciferase activity. Data are reported as the relative fold-increase compared with pGL3-Basic and represent the means ± SD of 3 replicates.

The firefly and *Renilla* activities were determined 48 h after the transfection using a dual luciferase assay kit (Promega) and a LB940 luminometer (Berthold, Bad Wildbad, Germany). The firefly activity was normalized to *Renilla* activity.

EMSA. Nuclear extract was prepared from OK cells transiently transfected with HNF-4α or not, according to the method of Shimakura et al. (37). The double-stranded oligonucleotides used in the EMSA are listed in Table 1. The OAT1 probes (−882/−853) and (−127/−100) were end-labeled with [γ-^{32}P]ATP using T4 polynucleotide kinase (Takara Bio) and purified through a Sephadex G-25 column (GE Healthcare). EMSA was performed according to Prieur et al. (32) but with some modifications. The OK nuclear extract (10 μg) was incubated in binding buffer [40 mM KCl, 10 mM Tris·HCl (pH 8.0), 1 mM DTT, 6% glycerol, and 0.05% Nonidet P-40] for 10 min at 4°C. Thereafter, one of the labeled probes was added and the mixture was incubated for a further 10 min at 4°C. For competition experiments and supershift assays, excess (50-fold) unlabeled oligonucleotides and antibody (2 μg) were added 10 min and 1 h before the addition of the labeled probe, respectively. The volume of the binding mixture was 20 μl throughout the experiment. The DNA-protein complex was then separated on a 4% polyacrylamide gel for 1.5 h at 200 V and room temperature in 0.5× Tris borate-EDTA buffer. Gels were dried and exposed to X-ray film for autoradiography.

Data analysis. The results were expressed relative to pGL3-Basic and represent the mean ± SD of three replicates. Two or three experiments were conducted, and representative results are shown.

RESULTS

Determination of the transcription start site of OAT1. To identify the transcription start site of human OAT1, 5′-RACE was performed. Sequencing of the longest RACE product showed that the terminal position of OAT1 cDNA was located 265 nucleotides above the start codon, which was 43 bp downstream of the 5′-end of OAT1 cDNA registered in the National Center for Biotechnology Information (NCBI) database (accession number NM_004790). No unreported intron was identified in the 5′-flanking region of OAT1, so the 5′-end of OAT1 cDNA registered in the NCBI database was numbered with +1 as the transcription start site in this study.

OAT1 promoter is transactivated by HNF-4α. To perform the functional analysis of the human OAT1 promoter, the 2,747-bp flanking region upstream of the transcription start site of OAT1 was subcloned into the pGL3-Basic vector. At first, the OAT1 promoter construct −2747/+88 was transiently transfected into a renal epithelial cell line derived from OK, a cell line derived from human embryonic kidney (HEK293), and a human intestinal cell line (Caco-2), and luciferase activity was measured. As shown in Fig. 1, the −2747/+88 construct showed a significant increase in luciferase activity compared with pGL3-Basic in OK cells, which have many characteristics of renal proximal tubule cells, including an organic anion transport system (17). However, this construct had little promoter activity in HEK293 and Caco-2 cells, which lack an organic anion transport system. Therefore, OK cells were used in the subsequent experiments.

Next, to investigate whether the OAT1 promoter is regulated by HNF-1α/β or HNF-4α, the −2747/+88 construct was transiently transfected into OK cells simultaneously with the HNF-1α, HNF-1β, or HNF-4α expression plasmid. Only HNF-4α could transactivate the OAT1 promoter activity markedly; HNF-1α and HNF-1β could not (Fig. 2). These results suggested that the OAT1 promoter is regulated by HNF-4α.

Identification of HNF-4α response elements. To determine the elements required for the transactivation of OAT1 promoter activity by HNF-4α, a series of deletion constructs of OAT1 were transfected into OK cells simultaneously with HNF-4α,

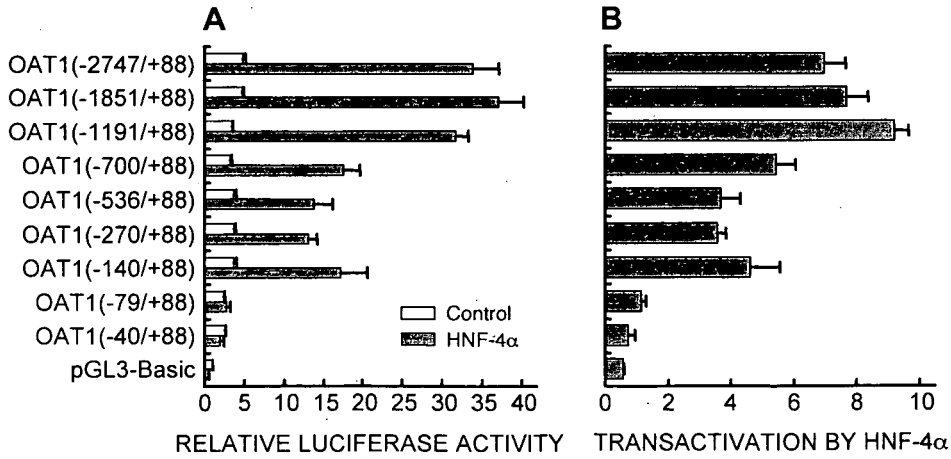

Fig. 3. Identification of the HNF-4α-responsive region in the human OAT1 promoter. A series of deleted promoter constructs [equimolar amounts of the −2747/+88 construct (500 ng)] and 500 ng of the HNF-4α expression vector or empty vector were transiently transfected into OK cells for luciferase assays. Firefly luciferase activity was normalized to *Renilla* luciferase activity. Data are reported as the relative fold-increase compared with pGL3-Basic (*A*) or as the ratio of HNF-4α expression vector to empty vector (*B*) and represent the means ± SD of 3 replicates.

and luciferase activity was measured (Fig. 3). With the −2747/+88 to −1191/+88 constructs, the promoter activity in the presence of HNF-4α increased seven- to ninefold compared with that in the absence of HNF-4α. Deletion of the fragment spanning −1191 to −700 bp reduced the activation of the OAT1 promoter by HNF-4α, and the −536/+88 to −140/+88 constructs showed the same level of activation by HNF-4α as the −700/+88 construct. Further deletion of the fragment spanning −140 to −79 bp almost abolished the responsiveness. These results suggested that the regions spanning −1191 to −700 and −140 to −79 bp contain the elements important for the transactivation of OAT1 promoter activity by HNF-4α.

HNF-4α binds as a homodimer to a DNA sequence consisting of a direct repeat of AGGTCA-like hexamers separated by one or two nucleotides, which were designated as DR-1 and DR-2, respectively (12, 21). We investigated whether the regions mentioned above had DR-1 and DR-2 sites using NUBIScan, an in silico tool to identify nuclear receptor response elements (29). As a result, a DR-2-like element was identified between −875 and −862 bp in the −1191/−700

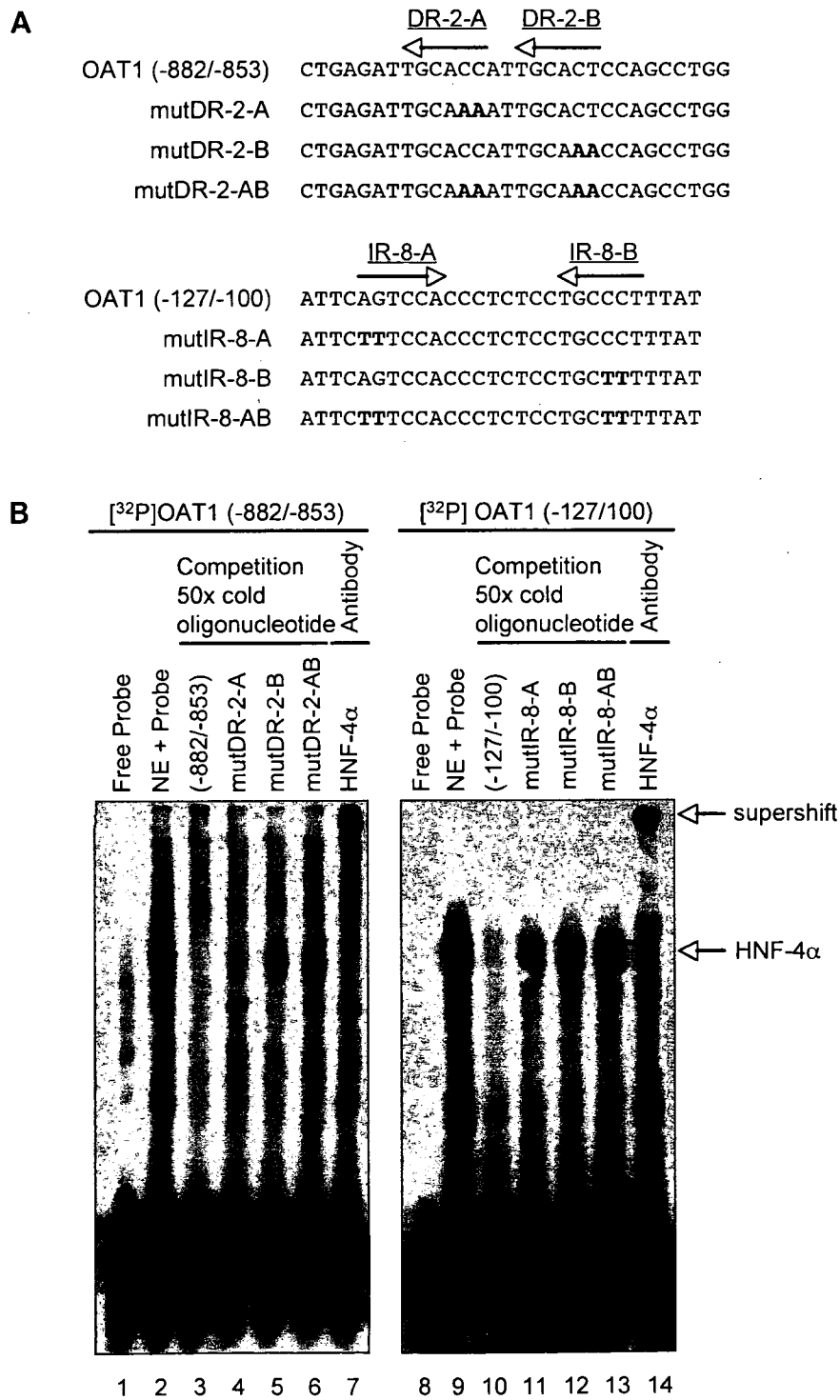

Fig. 4. EMSA using nuclear extract from OK cells transiently transfected with HNF-4α (OK-HNF-4α NE) and two human OAT1 probes, (−882/−853) and (−127/−100). *A*: sequence of the oligonucleotides used in EMSA. Mutations introduced into the oligonucleotides are shown in bold. *B*: OK-HNF-4α NE was incubated with the ^{32}P-labeled OAT1 oligonucleotide probe alone (*lanes 2* and *9*), or in the presence of excess unlabeled wild-type oligonucleotides (*lanes 3* and *10*), excess mutated oligonucleotides (*lanes 4–6* and *11–13*), or antibody against HNF-4α (*lanes 7* and *14*). In *lanes 1* and *8*, nuclear extract was not added.

fragment, while neither a DR-1 nor DR-2 site was found in the −140/−79 fragment. Between −123 and −104, however, the −140/−79 fragment contained an inverted repeat of hexamers separated by eight nucleotides (IR-8), which was recently identified as a HNF-4α response element in the human apolipoprotein AV promoter (32).

HNF-4α binds to DR-2 and IR-8 elements. To confirm that HNF-4α was able to bind to the DR-2 and IR-8 elements within the OAT1 promoter, EMSA was performed using an OAT1 probe (−882/−853) containing the DR-2 element or OAT1 probe (−127/−100) containing the IR-8 element and nuclear extract from OK cells transiently transfected with HNF-4α (OK-HNF-4α NE). Both OAT1 probes formed a DNA-protein complex (Fig. 4*B*, *lanes 2* and *9*), and the formation of the complex was completely impaired by the addition of an excess amount of the unlabeled wild-type oligonucleotides (Fig. 4*B*, *lanes 3* and *10*). Mutations in DR-2 (Fig. 4*A*, mutDR-2-B, mutDR-2-AB) and in IR-8 (Fig. 4*A*, mutIR-8-A, mutIR-8-B, mutIR-8-AB) abolished the ability to compete with the formation of the complex, while mutDR-2-A weakly competed with the formation of the complex (Fig. 4*B*, *lanes 4–6*, *11–13*). Furthermore, the DNA-protein complex was supershifted on the addition of the HNF-4α antibody (Fig. 4*B*, *lanes 7* and *14*). These results indicate that HNF-4α binds to DR-2 and IR-8 elements within the OAT1 promoter.

Mutagenesis of DR-2 and IR-8 elements. To examine the contribution of the DR-2 and IR-8 elements to the responsiveness to HNF-4α, mutations at these sites were introduced into the −2747/+88 construct, and OK cells were transfected. Mutations in DR-2-B and IR-8-B reduced the transactivation of OAT1 promoter activity by HNF-4α more than mutations in DR-2-A and IR-8-A, respectively (data not shown); hereafter, mutations in DR-2-B and IR-8-B are regarded as mutations in DR-2 and IR-8, respectively. As shown in Fig. 5, mutations in DR-2 and IR-8 reduced the responsiveness to HNF-4α to two-thirds and one-half of the wild-type level, respectively. Furthermore, mutations in both DR-2 and IR-8 reduced the responsiveness to one-third that of the wild-type. These results suggest that the DR-2 and IR-8 elements in the OAT1 promoter play an important role in the responsiveness to HNF-4α and that IR-8 contributed to the activation by HNF-4α more than did DR-2.

HNF-4α is responsible for basal OAT1 promoter activity. Focusing on the promoter activity in the absence of HNF-4α (Fig. 5), we found that mutations in IR-8 also reduced OAT1 promoter activity, suggesting that IR-8 is essential for basal promoter activity of OAT1. To investigate the influence of

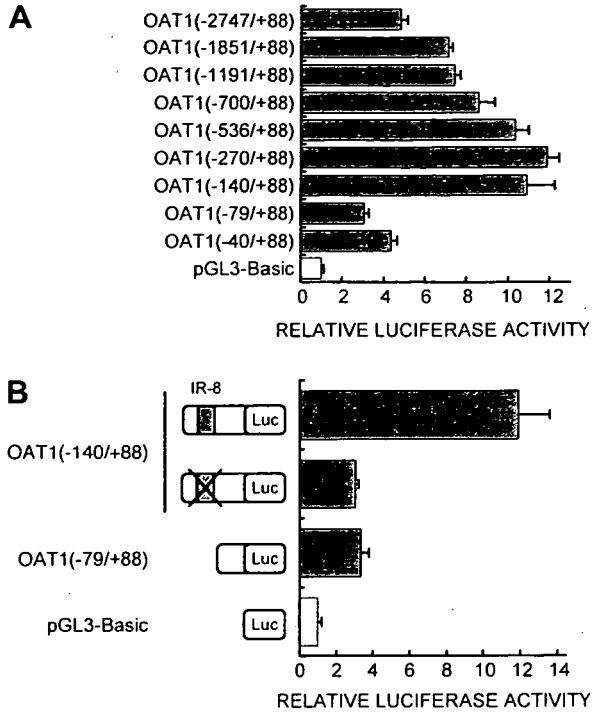

Fig. 6. Identification of the elements important for basal promoter activity of human OAT1. *A*: deletion analysis of the human OAT1 promoter in OK cells. A series of deleted promoter constructs [equimolar amounts of the −2747/+88 construct (500 ng)] were transfected into OK cells for luciferase assays. *B*: mutational analysis of the IR-8 in the human OAT1 promoter. The deleted or mutated constructs [equimolar amounts of the −140/+88 construct (330 ng)] were transfected into OK cells for luciferase assays. Firefly luciferase activity was normalized to *Renilla* luciferase activity. Data are reported as the relative fold-increase compared with pGL3-Basic and represent the means ± SD of 3 replicates. X, Presence of site-directed mutations.

IR-8 on basal activity, we carried out a progressive deletion analysis and a mutational analysis. Transfection of the −2747/+88 construct resulted in a fivefold increase in luciferase activity compared with that of pGL3-Basic, and serial 5′-deletions of the construct from −2747 to −1851, −1191, −700, −536, −270, and −140 gradually increased luciferase activity (Fig. 6*A*). However, deletion of the fragment spanning −140 to −79 bp significantly reduced the luciferase activity (Fig. 6*A*). These results suggested that the −140/−79 region containing IR-8 is essential for basal transcriptional activity.

Next, a mutation in IR-8 was introduced into the −140/+88 construct, and luciferase activity was measured. The mutation reduced luciferase activity to one-third of the wild-type level,

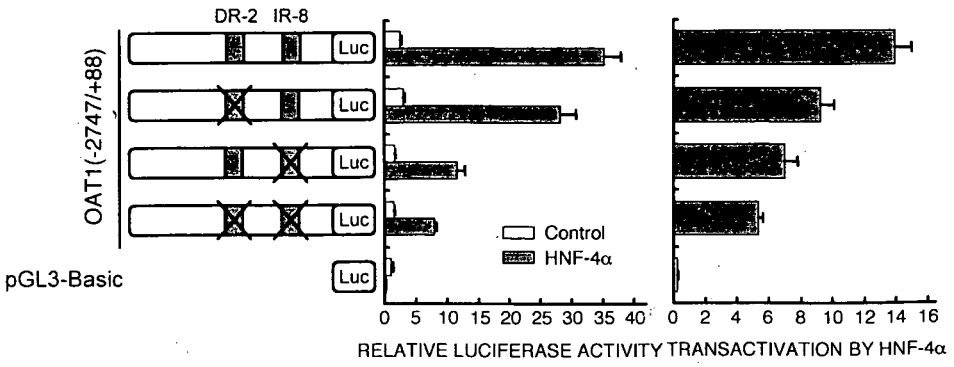

Fig. 5. Effects of mutation in the direct repeat (DR)-2 and inverted repeat (IR)-8 elements on the responsiveness to HNF-4α. The mutated −2747/+88 construct (500 ng) and 500 ng of the HNF-4α expression vector or empty vector were transiently transfected into OK cells for luciferase assays. Firefly luciferase activity was normalized to *Renilla* luciferase activity. Data are reported as the relative fold-increase compared with pGL3-Basic or as the ratio of HNF-4α expression vector to empty vector and represent the means ± SD of 3 replicates. X, Presence of site-directed mutations.

which was the same level of activity as the −79/+88 construct (Fig. 6*B*), suggesting that IR-8 is responsible for basal promoter activity of OAT1.

To examine whether endogenous HNF-4α binds to IR-8 without the overexpression of HNF-4α, EMSA was performed using an OAT1 probe (−127/−100) and nuclear extract from intact OK cells (OK-intact NE). Like OK-HNF-4α NE, OK-intact NE also formed a DNA-protein complex which was supershifted on the addition of the HNF-4α antibody (Fig. 7, *lanes 2* and *7*), suggesting that endogenous HNF-4α binds to IR-8 without the overexpression of HNF-4α. In competition experiments, mutIR-8-B and mutIR-8-AB did not impair the formation of the DNA-protein complex, while mutIR-8-A weakly competed with the formation of the complex (Fig. 7, *lanes 4–6*).

DISCUSSION

HNF-4α transactivates human OAT1 promoter activity, and this effect occurs mainly via DR-2 and IR-8 elements, as demonstrated by the deletion analysis, mutational analysis, and EMSA. Furthermore, it was found that HNF-4α is also responsible for basal promoter activity of OAT1 via IR-8 (Fig. 8). Prieur et al. (32) proposed that IR-8 is a novel HNF-4α response element, and our results support this. These findings may be useful for further understanding gene regulation by HNF-4α.

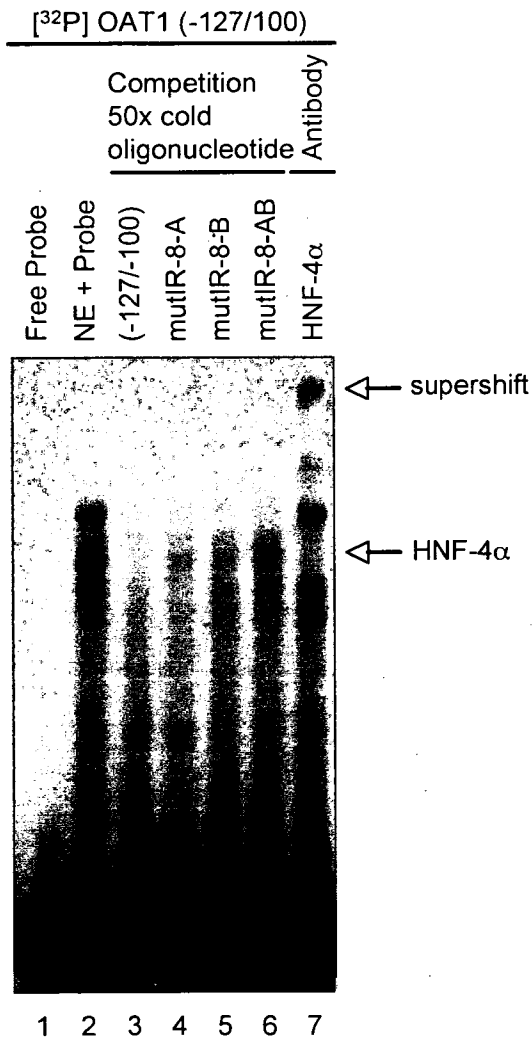

Fig. 7. EMSA using nuclear extract from intact OK cells (OK-intact NE) and a human OAT1 probe (−127/−100). OK-intact NE was incubated with the ^{32}P-labeled OAT1 oligonucleotide probe (−127/−100) alone (*lane 2*), or in the presence of excess unlabeled oligonucleotide (−127/−100; *lane 3*), excess mutated oligonucleotides (*lanes 4–6*), or antibody against HNF-4α (*lane 7*). In *lane 1*, nuclear extract was not added.

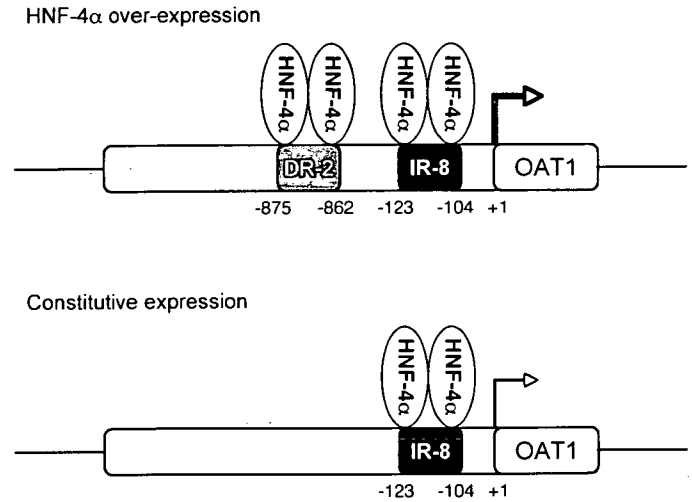

Fig. 8. Schematic model of transcriptional regulation of the human *OAT1* gene. In the abundance of HNF-4α, HNF-4α transactivates human OAT1 promoter activity via DR-2 and IR-8 elements. IR-8 contributes to the activation by HNF-4α more than DR-2 (HNF-4α overexpression). Under normal conditions, IR-8 is responsible for the basal promoter activity of OAT1, and HNF-4α binds to IR-8 (constitutive expression).

HNF-4α is an orphan member of the nuclear receptor superfamily that is expressed in the liver, kidney, intestine, stomach, and pancreas (27, 40). Liver-specific disruption of the *HNF-4α* gene indicated that HNF-4α is central to the maintenance of hepatocyte differentiation and lipid homeostasis (16). On the other hand, mutations in the gene encoding HNF-4α cause maturity-onset diabetes of the young (MODY), which is a genetically heterogeneous monogenic form of type 2 diabetes, associated with pancreatic β-cell dysfunction (46). In contrast to the roles of HNF-4α in the liver and pancreas, little has been reported on the physiological implications of HNF-4α in the kidney. In the present study, we clearly indicated that the renal *OAT1* gene is transcriptionally regulated by HNF-4α. Because HNF-4α and OAT1 protein showed the restricted intrarenal localization, that is, in the renal proximal tubular epithelial cells (22, 26), it is strongly suggested that HNF-4α is a key factor regulating the intrarenal expression of OAT1 protein.

In the EMSA using OK-HNF-4α NE, the mutDR-2-A oligonucleotide containing an intact DR-2-B competed more with the formation of the DNA-protein complex than did the mutDR-2-B oligonucleotide containing an intact DR-2-A (Fig. 4*B*, *lanes 4* and *5*). Similarly, in the EMSA using OK-intact NE, HNF-4α bound to the mutIR-8-A oligonucleotide containing an intact IR-8-B with higher affinity than the mutIR-8-B oligonucleotide containing an intact IR-8-A (Fig. 7, *lanes 4* and *5*). These results indicate that DR-2-B and IR-8-B had greater activity to bind HNF-4α than did DR-2-A and IR-8-A, respectively, which are consistent with the finding that mutations in DR-2-B and IR-8-B reduced the responsiveness to

HNF-4α more than mutations in DR-2-A and IR-8-A, respectively (data not shown). These findings suggest that DR-2-B and IR-8-B are important to the transactivation of the OAT1 promoter via HNF-4α compared with DR-2-A and IR-8-A. In the EMSA using OK-HNF-4α NE, both oligonucleotides mutIR-8-A and mutIR-8-B failed to impair the formation of the DNA-protein complex (Fig. 4*B*, *lanes 11* and *12*). It is possible that the abundance of HNF-4α caused the mutIR-8-A oligonucleotide to fail to completely compete with the formation of the complex.

It has been demonstrated that individual variation in the expression levels of drug transporters is responsible for the individual variation in pharmacokinetics by experiments using human tissue (15, 35, 36) and laboratory animals (11, 14, 20). Single nucleotide polymorphisms in the coding region [coding SNPs (cSNPs)] of drug transporter genes are also thought to be responsible for the variation in drug responses among individuals (19). Although there have been few reports on cSNPs of the human *OAT1* gene, allele frequencies of these cSNPs were very low (5, 13, 45). In addition, Fujita et al. (13) reported that there was no significant decrease in the renal secretory clearance of adefovir in subjects with R454Q, which resulted in a complete loss of OAT1 function in vitro. These reports suggest that cSNPs of human OAT1 are unlikely to influence the interindividual variation in the drug responses and that OAT1 expression is an alternative candidate for the cause of the variation in pharmacokinetics among individuals. Recent studies suggest that SNPs in the promoter region [regulatory SNPs (rSNPs)] can alter the transcription of genes (7). In the *OAT1* gene, Bhatnagar et al. (4) found one rSNP ~3 kb upstream of the transcription start site, but it is unclear whether this rSNP affects the mRNA level of OAT1. We previously reported that the OAT1 mRNA level varies and is significantly lower in the kidney of patients with renal diseases than in the normal kidney cortex (36). Accordingly, it is important to clarify the cause of the interindividual differences in OAT1 mRNA expression and the reduction in renal diseases. The present study suggests that HNF-4α regulates OAT1 expression at the mRNA level. Regulatory SNPs of OAT1, the HNF-4α expression level, or cSNPs in the *HNF-4α* gene that led to a loss of function may be the cause of the interindividual variation in OAT1 mRNA levels.

Tissue-specific gene expression is generally regulated by transcription factors (48). For example, we previously demonstrated that the intestine-specific transcription factor Cdx2 is responsible for the intestine-specific expression of H^+/peptide cotransporter 1 (38). OAT1 mRNA is mainly expressed in the kidney (1), and we found that HNF-4α is responsible for the transcriptional regulation of the *OAT1* gene. Interestingly, the major expression site of HNF-4α is the liver, but OAT1 mRNA is not expressed in the liver. Furthermore, the human *OCT1* gene is also under the control of HNF- 4α (34), but OCT1 mRNA is expressed in the liver but not in the kidney. Thus it is difficult to explain the renal-specific expression of OAT1 by HNF-4α itself. Other transcription factors that suppress the hepatic expression of OAT1 (or renal expression of OCT1) may contribute to tissue-specific expression. Alternatively, microRNA and DNA methylation of the promoter may be involved in the tissue-specific expression of genes (39, 44). Further studies are needed to elucidate the mechanism of tissue-specific expression of the SLC22A family.

In conclusion, the present study indicates that the human *OAT1* gene is regulated by HNF-4α. This is the first report on the transcriptional regulation of *OAT1*. In addition, *OAT1* is the first gene in the kidney whose promoter activity has been demonstrated to be regulated by HNF-4α.

ACKNOWLEDGMENTS

We thank Dr. Marco Pontoglio (Institute Pasteur, Paris, France) for kindly providing the human HNF-1α and HNF-1β expression vectors.

GRANTS

This work was supported in part by the 21st Century COE program "Knowledge Information Infrastructure for Genome Science," a Grant-in-Aid for Scientific Research from the Ministry of Education, Culture, Sports, Science, and Technology of Japan, and a Grant-in-Aid for Research on Advanced Medical Technology from the Ministry of Health, Labor and Welfare of Japan. J. Asaka is supported as a research assistant by the 21st Century COE program "Knowledge Information Infrastructure for Genome Science."

REFERENCES

1. **Anzai N, Kanai Y, Endou H.** Organic anion transporter family: current knowledge. *J Pharmacol Sci* 100: 411–426, 2006.
2. **Bahn A, Prawitt D, Buttler D, Reid G, Enklaar T, Wolff NA, Ebbinghaus C, Hillemann A, Schulten HJ, Gunawan B, Fuzesi L, Zabel B, Burckhardt G.** Genomic structure and in vivo expression of the human organic anion transporter 1 (hOAT1) gene. *Biochem Biophys Res Commun* 275: 623–630, 2000.
3. **Baumhueter S, Mendel DB, Conley PB, Kuo CJ, Turk C, Graves MK, Edwards CA, Courtois G, Crabtree GR.** HNF-1 shares three sequence motifs with the POU domain proteins and is identical to LF-B1 and APF. *Genes Dev* 4: 372–379, 1990.
4. **Bhatnagar V, Xu G, Hamilton BA, Truong DM, Eraly SA, Wu W, Nigam SK.** Analyses of 5′ regulatory region polymorphisms in human SLC22A6 (OAT1) and SLC22A8 (OAT3). *J Hum Genet* 51: 575–580, 2006.
5. **Bleasby K, Hall LA, Perry JL, Mohrenweiser HW, Pritchard JB.** Functional consequences of single nucleotide polymorphisms in the human organic anion transporter hOAT1 (SLC22A6). *J Pharmacol Exp Ther* 314: 923–931, 2005.
6. **Brandoni A, Villar SR, Picena JC, Anzai N, Endou H, Torres AM.** Expression of rat renal cortical OAT1 and OAT3 in response to acute biliary obstruction. *Hepatology* 43: 1092–1100, 2006.
7. **Buckland PR.** The importance and identification of regulatory polymorphisms and their mechanisms of action. *Biochim Biophys Acta* 1762: 17–28, 2006.
8. **Burckhardt BC, Burckhardt G.** Transport of organic anions across the basolateral membrane of proximal tubule cells. *Rev Physiol Biochem Pharmacol* 146: 95–158, 2003.
9. **Cheret C, Doyen A, Yaniv M, Pontoglio M.** Hepatocyte nuclear factor 1α controls renal expression of the Npt1-Npt4 anionic transporter locus. *J Mol Biol* 322: 929–941, 2002.
10. **De Simone V, De Magistris L, Lazzaro D, Gerstner J, Monaci P, Nicosia A, Cortese R.** LFB3, a heterodimer-forming homeoprotein of the LFB1 family, is expressed in specialized epithelia. *EMBO J* 10: 1435–1443, 1991.
11. **Deguchi T, Takemoto M, Uehara N, Lindup WE, Suenaga A, Otagiri M.** Renal clearance of endogenous hippurate correlates with expression levels of renal organic anion transporters in uremic rats. *J Pharmacol Exp Ther* 314: 932–938, 2005.
12. **Fraser JD, Martinez V, Straney R, Briggs MR.** DNA binding and transcription activation specificity of hepatocyte nuclear factor 4. *Nucleic Acids Res* 26: 2702–2707, 1998.
13. **Fujita T, Brown C, Carlson EJ, Taylor T, de la Cruz M, Johns SJ, Stryke D, Kawamoto M, Fujita K, Castro R, Chen CW, Lin ET, Brett CM, Burchard EG, Ferrin TE, Huang CC, Leabman MK, Giacomini KM.** Functional analysis of polymorphisms in the organic anion transporter, SLC22A6 (OAT1). *Pharmacogenet Genomics* 15: 201–209, 2005.
14. **Habu Y, Yano I, Okuda M, Fukatsu A, Inui K.** Restored expression and activity of organic ion transporters rOAT1, rOAT3 and rOCT2 after hyperuricemia in the rat kidney. *Biochem Pharmacol* 69: 993–999, 2005.

15. **Hashida T, Masuda S, Uemoto S, Saito H, Tanaka K, Inui K.** Pharmacokinetic and prognostic significance of intestinal MDR1 expression in recipients of living-donor liver transplantation. *Clin Pharmacol Ther* 69: 308–316, 2001.
16. **Hayhurst GP, Lee YH, Lambert G, Ward JM, Gonzalez FJ.** Hepatocyte nuclear factor 4α (nuclear receptor 2A1) is essential for maintenance of hepatic gene expression and lipid homeostasis. *Mol Cell Biol* 21: 1393–1403, 2001.
17. **Hori R, Okamura M, Takayama A, Hirozane K, Takano M.** Transport of organic anion in the OK kidney epithelial cell line. *Am J Physiol Renal Fluid Electrolyte Physiol* 264: F975–F980, 1993.
18. **Inui K, Masuda S, Saito H.** Cellular and molecular aspects of drug transport in the kidney. *Kidney Int* 58: 944–958, 2000.
19. **Ishikawa T, Tsuji A, Inui K, Sai Y, Anzai N, Wada M, Endou H, Sumino Y.** The genetic polymorphism of drug transporters: functional analysis approaches. *Pharmacogenomics* 5: 67–99, 2004.
20. **Ji L, Masuda S, Saito H, Inui K.** Down-regulation of rat organic cation transporter rOCT2 by 5/6 nephrectomy. *Kidney Int* 62: 514–524, 2002.
21. **Jiang G, Nepomuceno L, Hopkins K, Sladek FM.** Exclusive homodimerization of the orphan receptor hepatocyte nuclear factor 4 defines a new subclass of nuclear receptors. *Mol Cell Biol* 15: 5131–5143, 1995.
22. **Jiang S, Tanaka T, Iwanari H, Hotta H, Yamashita H, Kumakura J, Watanabe Y, Uchiyama Y, Aburatani H, Hamakubo T, Kodama T, Naito M.** Expression and localization of P1 promoter-driven hepatocyte nuclear factor-4α (HNF4α) isoforms in human and rats. *Nucl Recept* 1: 5, 2003.
23. **Kikuchi R, Kusuhara H, Hattori N, Shiota K, Kim I, Gonzalez FJ, Sugiyama Y.** Regulation of the expression of human organic anion transporter 3 by hepatocyte nuclear factor 1α/β and DNA methylation. *Mol Pharmacol* 70: 887–896, 2006.
24. **Maher JM, Slitt AL, Callaghan TN, Cheng X, Cheung C, Gonzalez FJ, Klaassen CD.** Alterations in transporter expression in liver, kidney, and duodenum after targeted disruption of the transcription factor HNF1α. *Biochem Pharmacol* 72: 512–522, 2006.
25. **Monica Torres A, Mac Laughlin M, Muller A, Brandoni A, Anzai N, Endou H.** Altered renal elimination of organic anions in rats with chronic renal failure. *Biochim Biophys Acta* 1740: 29–37, 2005.
26. **Motohashi H, Sakurai Y, Saito H, Masuda S, Urakami Y, Goto M, Fukatsu A, Ogawa O, Inui K.** Gene expression levels and immunolocalization of organic ion transporters in the human kidney. *J Am Soc Nephrol* 13: 866–874, 2002.
27. **Nakhei H, Lingott A, Lemm I, Ryffel GU.** An alternative splice variant of the tissue specific transcription factor HNF4α predominates in undifferentiated murine cell types. *Nucleic Acids Res* 26: 497–504, 1998.
28. **Ogasawara K, Terada T, Asaka J, Katsura T, Inui K.** Human organic anion transporter 3 gene is regulated constitutively and inducibly via a cAMP-response element. *J Pharmacol Exp Ther* 319: 317–322, 2006.
29. **Podvinec M, Kaufmann MR, Handschin C, Meyer UA.** NUBIScan, an in silico approach for prediction of nuclear receptor response elements. *Mol Endocrinology* 16: 1269–1279, 2002.
30. **Pontoglio M, Prie D, Cheret C, Doyen A, Leroy C, Froguel P, Velho G, Yaniv M, Friedlander G.** HNF1α controls renal glucose reabsorption in mouse and man. *EMBO Rep* 1: 359–365, 2000.
31. **Popowski K, Eloranta JJ, Saborowski M, Fried M, Meier PJ, Kullak-Ublick GA.** The human organic anion transporter 2 gene is transactivated by hepatocyte nuclear factor-4α and suppressed by bile acids. *Mol Pharmacol* 67: 1629–1638, 2005.
32. **Prieur X, Schaap FG, Coste H, Rodriguez JC.** Hepatocyte nuclear factor-4α regulates the human apolipoprotein AV gene: identification of a novel response element and involvement in the control by peroxisome proliferator-activated receptor-γ coactivator-1α, AMP-activated protein kinase, and mitogen-activated protein kinase pathway. *Mol Endocrinology* 19: 3107–3125, 2005.
33. **Russel FG, Masereeuw R, van Aubel RA.** Molecular aspects of renal anionic drug transport. *Annu Rev Physiol* 64: 563–594, 2002.
34. **Saborowski M, Kullak-Ublick GA, Eloranta JJ.** The human organic cation transporter-1 gene is transactivated by hepatocyte nuclear factor-4α. *J Pharmacol Exp Ther* 317: 778–785, 2006.
35. **Sakurai Y, Motohashi H, Ogasawara K, Terada T, Masuda S, Katsura T, Mori N, Matsuura M, Doi T, Fukatsu A, Inui K.** Pharmacokinetic significance of renal OAT3 (SLC22A8) for anionic drug elimination in patients with mesangial proliferative glomerulonephritis. *Pharm Res* 22: 2016–2022, 2005.
36. **Sakurai Y, Motohashi H, Ueo H, Masuda S, Saito H, Okuda M, Mori N, Matsuura M, Doi T, Fukatsu A, Ogawa O, Inui K.** Expression levels of renal organic anion transporters (OATs) and their correlation with anionic drug excretion in patients with renal diseases. *Pharm Res* 21: 61–67, 2004.
37. **Shimakura J, Terada T, Katsura T, Inui K.** Characterization of the human peptide transporter PEPT1 promoter: Sp1 functions as a basal transcriptional regulator of human PEPT1. *Am J Physiol Gastrointest Liver Physiol* 289: G471–G477, 2005.
38. **Shimakura J, Terada T, Shimada Y, Katsura T, Inui K.** The transcription factor Cdx2 regulates the intestine-specific expression of human peptide transporter 1 through functional interaction with Sp1. *Biochem Pharmacol* 71: 1581–1588, 2006.
39. **Shiota K.** DNA methylation profiles of CpG islands for cellular differentiation and development in mammals. *Cytogenet Genome Res* 105: 325–334, 2004.
40. **Sladek FM, Zhong WM, Lai E, Darnell JE Jr.** Liver-enriched transcription factor HNF-4 is a novel member of the steroid hormone receptor superfamily. *Genes Dev* 4: 2353–2365, 1990.
41. **Sweet DH.** Organic anion transporter (Slc22a) family members as mediators of toxicity. *Toxicol Appl Pharmacol* 204: 198–215, 2005.
42. **Terada T, Inui K.** Gene expression and regulation of drug transporters in the intestine and kidney. *Biochem Pharmacol* 73: 440–449, 2007.
43. **Villar SR, Brandoni A, Anzai N, Endou H, Torres AM.** Altered expression of rat renal cortical OAT1 and OAT3 in response to bilateral ureteral obstruction. *Kidney Int* 68: 2704–2713, 2005.
44. **Wienholds E, Plasterk RH.** MicroRNA function in animal development. *FEBS Lett* 579: 5911–5922, 2005.
45. **Xu G, Bhatnagar V, Wen G, Hamilton BA, Eraly SA, Nigam SK.** Analyses of coding region polymorphisms in apical and basolateral human organic anion transporter (OAT) genes [OAT1 (NKT), OAT2, OAT3, OAT4, URAT (RST)]. *Kidney Int* 68: 1491–1499, 2005.
46. **Yamagata K, Furuta H, Oda N, Kaisaki PJ, Menzel S, Cox NJ, Fajans SS, Signorini S, Stoffel M, Bell GI.** Mutations in the hepatocyte nuclear factor-4α gene in maturity-onset diabetes of the young (MODY1). *Nature* 384: 458–460, 1996.
47. **You G.** Towards an understanding of organic anion transporters: structure-function relationships. *Med Res Rev* 24: 762–774, 2004.
48. **Yu X, Lin J, Zack DJ, Qian J.** Computational analysis of tissue-specific combinatorial gene regulation: predicting interaction between transcription factors in human tissues. *Nucleic Acids Res* 34: 4925–4936, 2006.

BIOCHEMICAL PHARMACOLOGY 74 (2007) 161–168

available at www.sciencedirect.com

ScienceDirect

journal homepage: www.elsevier.com/locate/biochempharm

Interaction and transport characteristics of mycophenolic acid and its glucuronide via human organic anion transporters hOAT1 and hOAT3

Yuichi Uwai, Hideyuki Motohashi, Yoshie Tsuji, Harumasa Ueo, Toshiya Katsura, Ken-ichi Inui *

Department of Pharmacy, Kyoto University Hospital, Faculty of Medicine, Kyoto University, Shogoin, Sakyo-ku, Kyoto 606-8507, Japan

ARTICLE INFO

Article history:
Received 28 December 2006
Accepted 22 March 2007

Keywords:
Organic anion transporter
Mycophenolic acid
Mycophenolic acid glucuronide
Tubular secretion
Drug interaction

ABSTRACT

The immunosuppressant mycophenolate mofetil (MMF) is frequently administered with calcineurin inhibitors and corticosteroids to recipients of organ transplantations. However, the renal handling of the active metabolite mycophenolic acid (MPA) and 7-O-MPA-glucuronide (MPAG) has been unclear. The purpose of the present study was to assess the interaction of MPA and MPAG with the human renal organic anion transporters hOAT1 (SLC22A6) and hOAT3 (SLC22A8), by conducting uptake experiments using HEK293 cells stably expressing these transporters. MPA and MPAG inhibited the time-dependent uptake of *p*-[^{14}C]aminohippurate by hOAT1 and that of [^{3}H]estrone sulfate by hOAT3. The apparent 50% inhibitory concentration (IC_{50}) of MPA for hOAT1 and hOAT3 was estimated at 10.7 and 1.5 μM, respectively. In the case of MPAG, the IC_{50} values were calculated at 512.3 μM for hOAT1 and 69.1 μM for hOAT3. Eadie–Hofstee plot analyses showed that they inhibited hOAT1 noncompetitively and hOAT3 competitively. No inhibitory effects of tacrolimus, cyclosporin A and azathioprine on transport of *p*-[^{14}C]aminohippurate by hOAT1 and of [^{3}H]estrone sulfate by hOAT3 were observed. No transport of MPA by these transporters was observed. On the other hand, the uptake of MPAG into cells was stimulated by the expression of hOAT3, but not hOAT1. These findings propose the possibility that the administration of MMF decreases the renal clearance of drugs which are substrates of hOAT1 and hOAT3. Present data suggest that hOAT3 contributes to the renal tubular secretion of MPAG.

1. Introduction

An immunosuppressive agent, mycophenolate mofetil (MMF) is commonly prescribed with the calcineurin inhibitor tacrolimus or cyclosporin A and corticosteroids for patients who have received a solid organ transplantation. After orally administered and absorbed, MMF is converted to an active metabolite, mycophenolic acid (MPA; Fig. 1) by serum esterases. MPA is mainly excreted into urine after being metabolized to 7-O-MPA-glucuronide (MPAG) by the hepatic uridine diphosphate-glucuronosyltransferases [1,2]. The genetic variants of uridine diphosphate-glucuronosyltransferases contribute to the extensive variability in the pharmacokinetics of the immunosuppressant [3,4]. Furthermore, the enterohepatic circulation of MPAG/MPA exists, and tubular secretion as well as glomerular filtration is responsible for the

* *Corresponding author.* Tel.: +81 75 751 3577; fax: +81 75 751 4207.
E-mail address: inui@kuhp.kyoto-u.ac.jp (K.-i. Inui).

Abbreviations: MMF, mycophenolate mofetil; MPA, mycophenolic acid; MPAG, mycophenolic acid glucuronide; OAT, organic anion transporter

0006-2952/$ – see front matter © 2007 Elsevier Inc. All rights reserved.
doi:10.1016/j.bcp.2007.03.024

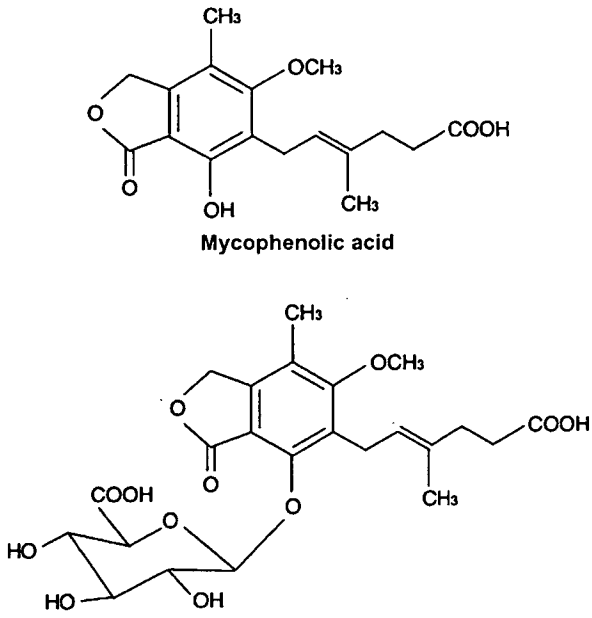

Fig. 1 – Chemical structure of mycophenolic acid and its glucuronide.

urinary excretion of MPAG [1]. Thus, the process by which MMF is eliminated, is very intricate.

Besides immunosuppressive agents, many drugs are given to recipients of organ transplantations, to prevent or treat infections, gastrointestinal ulcers, thrombus, ascites, pleural fluid, hypertension, diabetes, osteoporosis, gout, bronchitis and so on. Accordingly, side effects caused by drug interactions often occur. In addition to tacrolimus and cyclosporin A, MMF was shown to interact with various drugs. For instance, MMF reduced the renal clearance of acyclovir and ganciclovir, and the pharmacokinetics of MPA or MPAG were affected by cyclosporin A, glucocorticoids and non-steroidal anti-inflammatory drugs [1,5–8]. Taking these MPA and/or MPAG-mediated drug interactions into account, together with the complexity of the fate of MMF, it is important to identify the drug-metabolizing enzymes and drug transporters interacting with this immunosuppressive agent for a successful organ transplantation.

The human organic anion transporters (hOATs) mediate transport of clinically important drugs, such as diuretics, antibiotics, antivirals, histamine H_2 receptor antagonists, non-steroidal anti-inflammatory drugs and so on [9,10]. Among the family, hOAT1 (SLC22A6) and hOAT3 (SLC22A8) were shown to be predominantly expressed in the basolateral membrane of the renal proximal tubules [11], suggesting that they play main roles in the renal tubular uptake of organic compounds from blood. Furthermore, as previously reported [12], it is possible that hOAT1 and hOAT3 are targets of the interaction between methotrexate and non-steroidal anti-inflammatory drugs.

This background suggests that the renal organic anion transporters are concerned with the renal excretion of the metabolites of MMF and drug interaction with them, but to our knowledge, no report has examined the interaction of MPA and MPAG with the renal organic anion transporters at a molecular level. In the present study, the inhibitory effects of MPA and MPAG on hOAT1 and hOAT3 were assessed. In addition, the contribution of hOAT1 and hOAT3 to the renal tubular secretion of MPA and MPAG was investigated.

2. Materials and methods

2.1. Materials

p-[glycyl-1-^{14}C]Aminohippurate (1.9 GBq/mmol) and [6,7-^{3}H(N)]estrone sulfate, ammonium salt (2.1 TBq/mmol) were obtained from NEN™ Life Science Products Inc. (Boston, MA, USA) and Perkin-Elmer Life Sciences Inc. (Boston, MA, USA), respectively. MPA and its glucuronide were from Wako Pure Chemical Industries (Osaka, Japan) and Analytical Services International Ltd. (London, UK), respectively. Tacrolimus and cyclosporin A were kindly supplied by Fujisawa Pharmaceutical (Newly, Astellas Pharma Inc., Tokyo, Japan) and Novartis Pharma KK, Co. Ltd. (Tokyo, Japan), respectively. Azathioprine and unlabelled estrone sulfate, sodium salt and probenecid were purchased from Sigma (St. Louis, MO, USA). All other chemicals used were of the highest purity available.

2.2. Uptake of *p*-[^{14}C]aminohippurate and [^{3}H]estrone sulfate by HEK293 cells stably expressing hOAT1 and hOAT3

According to our former report [13], experiments on the uptake of *p*-[^{14}C]aminohippurate and [^{3}H]estrone sulfate were performed using HEK293 cells stably transfected with a pBK-CMV vector containing hOAT1 cDNA, hOAT3 cDNA or no cDNA, named HEK-hOAT1, HEK-hOAT3 and HEK-pBK, respectively. In brief, 48 h after the cells were seeded on poly-D-lysine-coated 24-well plates at a density of 2×10^5 cells/well, the accumulation of *p*-[^{14}C]aminohippurate or [^{3}H]estrone sulfate by the cells was examined. The composition of the incubation medium was as follows: 145 mM NaCl, 3 mM KCl, 1 mM $CaCl_2$, 0.5 mM $MgCl_2$, 5 mM D-glucose and 5 mM HEPES (pH 7.4). After the preincubation of the cells with 0.2 ml of the incubation medium at 37 °C for 10 min, the medium was replaced with 0.2 ml of incubation medium containing test compounds. At the end of the incubation, the medium was aspirated and then the cells were washed twice with 1 ml of ice-cold incubation medium. The cells were lysed in 250 μl of 0.5N NaOH solution, and the radioactivity in aliquots was determined in 3 ml of ACSII (Amersham International, Buckinghamshire, UK). The protein contents of the solubilized cells were determined by the method of Bradford using the Bio-Rad protein assay kit (Bio-Rad, Hercules, CA, USA) with bovine γ-globulin as a standard.

2.3. Uptake of MPA and MPAG by HEK293 cells stably expressing hOAT1 and hOAT3

Forty-eight hours after the cells were seeded on poly-D-lysine-coated 12-well plates at a density of 4×10^5 cells/well, the amounts of MPA and MPAG taken up by the cells were

examined. After the uptake, experiments were performed as described above, the cells were scraped off with a rubber policeman into 300 μl of 50% acetonitrile in 20 mM phosphate buffer (pH 3.0) and maintained for 30 min at room temperature. The extract solution was centrifuged at 14,000 rpm (Centrifuge 5417C, eppendorf, Hamburg, Germany) for 20 min. The supernatant was filtered through a Cosmonice Filter W (0.45 μm; Nacalai Tesque, Kyoto, Japan) and analyzed by high-performance liquid chromatography. The protein contents of the cells solubilized in 200 μl of 0.5N NaOH were determined.

2.4. *Analytical method for MPA and MPAG*

The amounts of MPA and MPAG in the extract solution were measured using a high-performance liquid chromatograph (LC-10AS, Shimadzu Co., Kyoto, Japan) equipped with a UV spectrophotometric detector (SPD-10AV, Shimadzu Co.) and an integrator (Chromatopac C-R6A, Shimadzu Co.) under the following conditions: column, TSK-GEL ODS-80^{TM}, 4.6 mm × 250 mm (TOSOH Co., Tokyo, Japan); flow rate, 0.8 ml/min; temperature, 40 °C; wavelength, 254 nm for both compounds; mobile phase, 40% acetonitrile in 20 mM phosphate buffer (pH 3.0) for MPA, 30% acetonitrile in 20 mM phosphate buffer (pH 3.0) for MPAG. When the calibration curve of MPA was depicted from 50 to 500 nM, the linearity was observed. In the case of MPAG, the standard curve showed the linearity ranged from 40 to 400 nM. The concentration of all samples was within the range.

2.5. *Statistical analysis*

Data were statistically analyzed with a one-way analysis of variance followed by Scheffe's test using StatView (SAS Institute Inc., NC, USA).

3. Results

3.1. *Inhibitory effects of MPA and MPAG on hOAT1 and hOAT3*

First, to examine whether MPA and MPAG interact with hOAT1 and hOAT3, the effects of MPA and MPAG on the time-dependent uptake of *p*-[^{14}C]aminohippurate by HEK-hOAT1 and of [^{3}H]estrone sulfate by HEK-hOAT3 were investigated. As shown in Fig. 2A, the amount of *p*-[^{14}C]aminohippurate taken up by HEK-hOAT1 increased linearly for 2 min. MPA at 300 μM completely inhibited the hOAT1-mediated transport of *p*-[^{14}C]aminohippurate. MPAG at 300 μM also inhibited the uptake of *p*-[^{14}C]aminohippurate by hOAT1, but the inhibitory effect was weaker. A similar phenomenon was observed for their inhibitory effects on hOAT3 (Fig. 2B). No linearity in the uptake of [^{3}H]estrone sulfate by hOAT3 was detected. Subsequent uptake experiments using *p*-[^{14}C]aminohippurate and [^{3}H]estrone sulfate were performed with an incubation time of 2 min for hOAT1 and 1 min for hOAT3.

Next, the concentration-dependence of the inhibitory effects of MPA and MPAG on hOAT1 and hOAT3 was investigated. Fig. 3 is representative of three independent

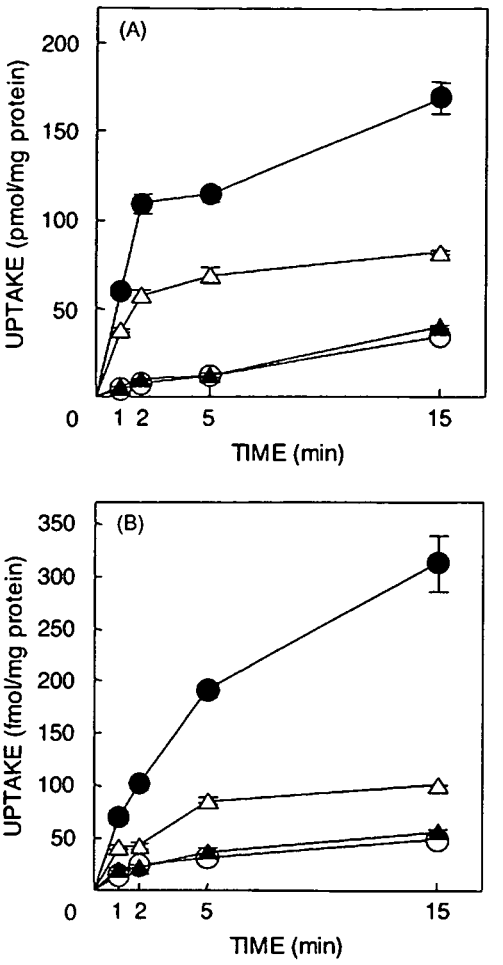

Fig. 2 – Time-dependent uptake of *p*-[^{14}C]aminohippurate by hOAT1 (A) and [^{3}H]estrone sulfate by hOAT3 (B) in the presence of MPA and MPAG. (A) HEK-pBK (open circle) and HEK-hOAT1 were incubated with 5 μM *p*-[^{14}C]aminohippurate for the indicated period in the absence (closed circle) or presence of MPA (closed triangle) and MPAG (open triangle) at 300 μM. (B) HEK-pBK (open circle) and HEK-hOAT3 were incubated with 17.5 nM [^{3}H]estrone sulfate for the indicated period in the absence (closed circle) or presence of MPA (closed triangle) and MPAG (open triangle) at 300 μM. Each point represents the mean ± S.E. of the uptake of *p*-[^{14}C]aminohippurate or [^{3}H]estrone sulfate in three monolayers.

experiments. The apparent 50% inhibitory concentration (IC_{50}) of MPA and MPAG were estimated to be 10.7 and 512.3 μM for hOAT1, and 1.5 and 69.1 μM for hOAT3, respectively (Table 1). It was elucidated that MPA inhibited hOAT1 and hOAT3 to a greater extent than MPAG, and that the inhibitory effects of MPA and MPAG on hOAT3 were more potent than those on hOAT1.

In order to clarify the inhibition modes of MPA and MPAG, effects of MPA and MPAG on concentration-dependent uptake of *p*-[^{14}C]aminohippurate by hOAT1 and of [^{3}H]estrone sulfate by hOAT3 were examined and Eadie-Hofstee plot analysis was conducted (Fig. 4). Based on the

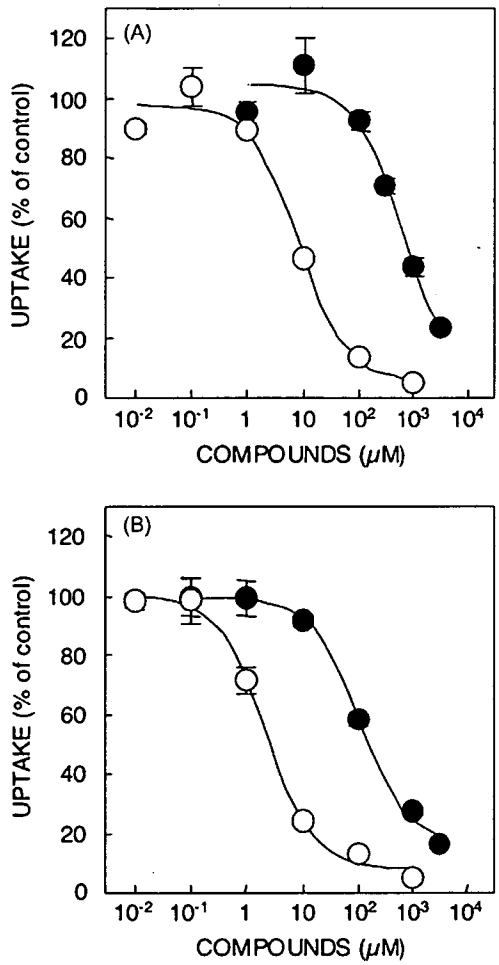

Fig. 3 – Dose-dependent effect of MPA and MPAG on hOAT1 (A) and hOAT3 (B). (A) HEK-hOAT1 was incubated with 5 μM *p*-[^{14}C]aminohippurate for 2 min in the absence (control) or presence of MPA (open circle) and MPAG (closed circle) at various concentrations. (B) HEK-hOAT3 was incubated with 17.5 nM [^{3}H]estrone sulfate for 1 min in the absence (control) or presence of MPA (open circle) and MPAG (closed circle) at various concentrations. Each point represents the mean ± S.E. of the uptake of *p*-[^{14}C]aminohippurate or [^{3}H]estrone sulfate in three monolayers.

three separate experiments, V_{max} values of *p*-[^{14}C]aminohippurate uptake by hOAT1 were significantly reduced in the presence of MPA and MPAG (control: 750.9 ± 44.9 pmol/mg protein/2 min; with MPA: 416.1 ± 28.7 pmol/mg protein/2 min; with MPAG: 476.5 ± 51.8 pmol/mg protein/2 min, mean ± S.E.) and K_m values were not changed (control: 34.2 ± 2.4 μM; with MPA: 34.8 ± 9.0 μM; with MPAG: 50.7 ± 12.6 μM). On the other hand, they significantly increased K_m values of hOAT3-mediated transport of [^{3}H]estrone sulfate (control: 13.2 ± 2.5 μM; with MPA: 54.0 ± 9.6 μM; with MPAG: 61.3 ± 9.6 μM, mean ± S.E.) and did not affect V_{max} values (control: 76.1 ± 9.8 pmol/mg protein/min; with MPA: 79.3 ± 11.6 pmol/mg protein/min; with MPAG: 63.7 ± 6.1 pmol/mg protein/min). These findings indicate that the inhibition manner of MPA and MPAG is noncompetitive for hOAT1 and competitive for hOAT3.

Table 1 – The IC_{50} values of MPA and MPAG for the uptake of *p*-[^{14}C]aminohippurate by hOAT1 and [^{3}H]estrone sulfate by hOAT3

	IC_{50} value (μM)	
	MPA	MPAG
hOAT1	10.7 ± 1.7	512.3 ± 109.7
hOAT3	1.5 ± 0.4	69.1 ± 23.2

HEK-hOAT1 and HEK-hOAT3 were incubated with 5 μM *p*-[^{14}C]aminohippurate for 2 min and 17.5 nM [^{3}H]estrone sulfate for 1 min, respectively, in the absence or presence of MPA or MPAG at various concentrations. The IC_{50} values were estimated by a nonlinear regression analysis of competition curves with one compartment with the following equation: uptake amount = (uptake amount without MPA and MPAG) × IC_{50}/(IC_{50} + [concentration of MPA or MPAG]) + (hOAT-independent uptake amount). The values represent the mean ± S.E. of three separate experiments.

3.2. *Effect of other immunosuppressive drugs on hOAT1 and hOAT3*

In addition to MPA and MPAG, the influences of other immunosuppressants, such as tacrolimus, cyclosporin A and azathioprine on hOAT1 and hOAT3 were assessed. Significant inhibition by these immunosuppressive agents was not observed (Table 2). These results indicate that tacrolimus, cyclosporin A and azathioprine do not interact with hOAT1 and hOAT3. The residue uptake amounts of *p*-[^{14}C]aminohippurate and [^{3}H]estrone sulfate in the presence of MPA at 300 μM were considered to be hOAT-independent uptake.

Table 2 – Effect of various immunosuppressants on the uptake of *p*-[^{14}C]aminohippurate by hOAT1 and [^{3}H]estrone sulfate by hOAT3

	Uptake (% of control)	
	hOAT1	hOAT3
HEK-pBK	6.7 ± 0.2*	11.3 ± 0.9*
Control	100 ± 10.6	100 ± 6.0
DMSO (0.1%)	86.4 ± 5.7	99.7 ± 0.9
Tacrolimus (1 μM)	92.7 ± 2.3	87.4 ± 2.5
Cyclosporin A (1 μM)	96.4 ± 1.2	105.2 ± 3.4
Azathioprine (10 μM)	95.4 ± 4.3	81.6 ± 3.6
MPA (300 μM)	10.8 ± 0.5*	14.6 ± 1.8*
MPAG (300 μM)	44.5 ± 2.4*	24.0 ± 1.9*

HEK-hOAT1 and HEK-hOAT3 were incubated with 5 μM *p*-[^{14}C]aminohippurate for 2 min and 17.5 nM [^{3}H]estrone sulfate for 1 min, respectively, in the absence (control) or presence of dimethylsulphoxide (DMSO), tacrolimus, cyclosporin A, azathioprine, MPA or MPAG at the indicated concentrations. Each value represents the mean ± S.E. of the uptake of *p*-[^{14}C]aminohippurate by hOAT1 and [^{3}H]estrone sulfate by hOAT3 in three monolayers. Test solutions with tacrolimus, cyclosporine A and azathioprine contained DMSO at less than 0.1%.
* $p < 0.0001$, significantly different from control.

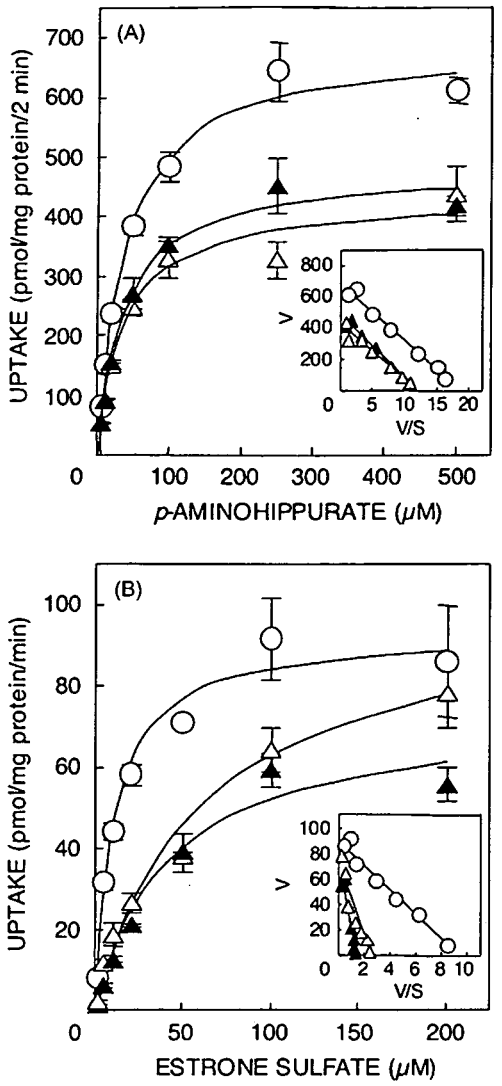

Fig. 4 – Effect of MPA and MPAG on kinetic parameters of p-[^{14}C]aminohippurate uptake by hOAT1 (A) and [^{3}H]estrone sulfate uptake by hOAT3 (B). (A) HEK-pBK and HEK-hOAT1 were incubated with p-[^{14}C]aminohippurate at various concentrations for 2 min in the absence or presence of 5 μM MPA and 200 μM MPAG and the hOAT1-mediated uptake of p-[^{14}C]aminohippurate was plotted in the figure (control: open circle; with MPA: open triangle; with MPAG: closed triangle). (B) HEK-pBK and HEK-hOAT3 were incubated with [^{3}H]estrone sulfate at various concentrations for 1 min in the absence or presence of 5 μM MPA and 200 μM MPAG and the hOAT3-mediated uptake of [^{3}H]estrone sulfate was plotted in the figure (control: open circle; with MPA: open triangle; with MPAG: closed triangle). Each point represents the mean ± S.E. of the uptake of p-[^{14}C]aminohippurate or [^{3}H]estrone sulfate in a typical experiments with three determinations. Insets represent Eadie–Hofstee plots of the uptake; V, uptake rate (pmol/mg protein/2 min for p-[^{14}C]aminohippurate uptake by hOAT1 and pmol/mg protein/min for [^{3}H]estrone sulfate uptake by hOAT3); S, concentration of p-[^{14}C]aminohippurate or [^{3}H]estrone sulfate (μM).

Table 3 – Amounts of MPA and MPAG taken up by HEK-hOAT1 and HEK-hOAT3

	Uptake (pmol/mg protein/h)		
	HEK-pBK	HEK-hOAT1	HEK-hOAT3
MPA	75.3 ± 4.1	81.2 ± 3.2	69.8 ± 5.6
MPAG	108.3 ± 9.7	165.3 ± 2.9	429.9 ± 30.7

HEK-pBK, HEK-hOAT1 and HEK-hOAT3 were incubated with 10 μM MPA or 400 μM MPAG for 1 h. The values represent the mean ± S.E. of the amounts of MPA and MPAG taken up by three monolayers. $p < 0.001$, significantly different from HEK-pBK.

3.3. *Uptake of MPA and MPAG by HEK-hOAT1 and HEK-hOAT3*

Finally, to examine whether hOAT1 and hOAT3 transport MPA and MPAG, the amounts of MPA and MPAG taken up by HEK-pBK, HEK-hOAT1 and HEK-hOAT3 were evaluated. As represented in Table 3, significant increases in the uptake of MPA with the expression of hOAT1 or hOAT3 were not detected. On the other hand, the amount of MPAG taken up by HEK-hOAT3 was significantly larger than that by HEK-pBK. The hOAT3-mediated uptake of MPAG was decreased to 61.1 and 62.8% in the presence of estrone sulfate and probenecid, respectively, at 100 μM. Although, the accumulation of MPAG by HEK-hOAT1 was greater than that by the control cells, the difference was not significant. These findings indicate that MPAG is a substrate of hOAT3.

4. Discussion

In organ transplantation, many drugs, including immunosuppressants, antibiotics, antivirals, antifungals, diuretics, histamine H_2 receptor antagonists, proton pump inhibitors, anticoagulants, bronchodilators and hypouricemic agents are administered to recipients. Accordingly, drugs should be prescribed with predictions of drug interactions [14]. To avoid adverse effects via drug interactions, information on the routes of elimination of a drug and its inhibitory effects on drug-metabolizing enzymes and drug transporters is required. The internal use of MMF causes a delay in the elimination of acyclovir [5]. Renal organic anion transporters are involved in the urinary excretion of acyclovir [15], suggesting that the interaction occurs via the renal organic anion transporters. However, the interaction between acyclovir and MMF has not been examined in detail. In addition, although many studies regarding uridine diphosphate-glucuronosyltransferases involved in the glucuronidation of MPA have been performed, there is no report showing the renal handling of MPA and MPAG. Against this background, we evaluated the inhibitory effects of MPA and MPAG on hOAT1 and hOAT3, which play important roles in the renal tubular secretion of various drugs, including acyclovir [16,17]. In addition, the contribution of hOAT1 and hOAT3 to the tubular secretion of MPA and MPAG was investigated.

The present study shows that MPA and MPAG inhibited hOAT1 and hOAT3 (Fig. 2), and that the inhibitory effects of MPA on both transporters were much stronger than those of

MPAG (Fig. 3). The IC_{50} values of MPA for hOAT1 and hOAT3 were estimated to be 10.7 and 1.5 μM, respectively. According to Bullingham et al. [18], the maximum plasma concentration of MPA reached 34.0 μg/ml (106 μM) when 1.5 g of MMF was administered in healthy volunteers. MPA strongly binds to serum albumin, and the free fraction of MPA in blood is 1–3% at normal albumin levels [1]. Taking these findings into consideration, together with the IC_{50} values of MPA for hOAT1 and hOAT3, these transporters should be moderately inhibited by unbound MPA in patients taking MMF. Furthermore, because MPA plasma profiles exhibit a sharp peak after the administration of MMF, it is speculated that the MPA-mediated inhibition of hOAT1 and hOAT3 would disappear 6 h after the dosing of MMF. However, Nowak and Shaw [19] reported that the free fraction of MPA was dramatically increased when albumin concentrations were below 20 g/l in vitro. There is a case report representing that the free level of MPA was enhanced up to 18.3% in a renal transplant recipient whose serum albumin level fell to less than 20 g/l, leading to myelosuppression [20]. Because the inhibition of hOAT1 and hOAT3 by free MPA is predicted to be marked in such a severe case of hypoalbuminemia, MPA-related drug interaction via hOAT1 and hOAT3 also should be considered.

One of the most important findings of the present study is that MPAG is a substrate of hOAT3, and no transport of MPA by hOAT1 and hOAT3 was observed (Table 3). The results are consistent with the disposition of MPA and MPAG. MPA is little excreted into urine, and the renal tubular secretion of MPAG is involved in its urinary excretion [1]. Our previous study showed that among the hOAT family, hOAT3 had the highest levels of mRNA in the kidney cortex [11]. Therefore, hOAT3 is considered to play a major role in the renal secretion of MPAG. In contrast, hardly any MPA is excreted into the urine. MPA is little filtrated through the glomerulus because of its extensive protein binding and is not transported by either hOAT1 or hOAT3. Therefore, MPA would not be transferred from blood to urine.

So far, MPAG has been regarded as the causative compound in acyclovir–MMF interaction, because MPAG as well as acyclovir is secreted into urine in the renal proximal tubules [5]. Acyclovir is a substrate of hOAT1 [16,17], suggesting that hOAT1 is, at least in part, involved in the drug interaction. The present study indicates that MPAG is an inhibitor of hOAT1 and hOAT3, but its inhibitory effects are not very strong (Fig. 3). It was reported that the maximum plasma concentration of MPAG in healthy subjects was 43.1 μg/ml (87 μM) when 1.5 g of MMF was administered [18]. In addition, the fact that 80% of the MPAG in blood binds to serum albumin suggests that the inhibition of hOAT1 and hOAT3 by MPAG would not be so prominent. However, a good correlation between the renal clearance of MPAG and glomerular filtration rate was observed, and the AUC of MPAG was increased in patients with impaired renal function [21]. Accordingly, MPAG-involved drug interaction via hOAT1 and hOAT3 would be frequently recognized in recipients with renal dysfunction. In addition, MPAG competes with MPA to bind proteins [19]. The accumulation of MPAG would lead to the enhancement of unbound MPA levels, and inhibition of hOAT1 and hOAT3 by MPA would be more potent in such a case. Furthermore, Kaplan et al. [22] suggested an unknown influence on the protein binding of MPA in patients with renal dysfunction besides the accumulation of MPAG. Renal disease is considered an important factor for MMF-related drug interaction via hOAT1 and hOAT3.

As represented in Fig. 4, it has been found that MPA and MPAG inhibit hOAT1 and hOAT3 in different manners. The noncompetitive inhibition of hOAT1 by MPA and MPAG may lead to no transport of these compounds by hOAT1 (Table 2). On the other hand, MPA and MPAG inhibited hOAT3 competitively, and only MPAG was transported by hOAT3. It is interesting that MPA is a potent competitive inhibiter of hOAT3 and is not transported by the transporter. Like MPA, several compounds, including probenecid, glibenclamide, ibuprofen and ketoprofen are shown to inhibit OAT1 strongly and not to be transported by OAT1 [23–25].

It seems that there is inter-individual variation in the interaction between acyclovir and MMF. Royer et al. [26] reported neutropenia in a patient taking valacyclovir and MMF. However, in the report of Gimenez et al. [5], a significant increase in the concentration of acyclovir was not observed in healthy volunteers using valacyclovir and MMF. Recently, we found extensive variability in mRNA levels of hOATs in the human kidney, and a correlation between the elimination rates of cefazolin and hOAT3 mRNA levels in renal biopsy specimens was recognized [27,28]. In addition to the hypoalbuminemia and renal failure described above, mRNA levels of hOATs are suggested to be related to the inter-individual variability of acyclovir–MMF interaction. At present, the application of therapeutic drug monitoring, when MMF is administered, is argued. In terms of the MMF-induced drug interaction via hOAT1 and hOAT3, the free levels of MPA also should be monitored in patients with hypoalbuminemia or renal failure.

Present study represented that other immunosuppressants, including tacrolimus, cyclosporin A and azathioprine did not inhibit hOAT1 and hOAT3 (Table 2). The clinical unbound ranges of tacrolimus, cyclosporin A and azathioprine were less than the concentrations used in this study. Accordingly, it is suggested that tacrolimus, cyclosporin A and azathioprin do not interfere with hOAT1 and hOAT3 in patients. They are extensively metabolized in the body [29–31]. We did not examine effects of their metabolites on hOAT1 and hOAT3, and the possibility that the metabolites inhibit hOAT1 and hOAT3 has remained.

In summary, the present study shows that MPA and MPAG inhibit hOAT1 and hOAT3, and that the inhibitory effects of MPA on the transporters were much stronger than those of MPAG. From their IC_{50} values for these transporters and normal free levels of MPA and MPAG in plasma, it is considered that there is no need to pay too much attention to the inhibition of hOAT1 and hOAT3 by MPA and MPAG. However, in patients with hypoalbuminemia or renal impairment, care should be taken to avoid MMF-related drug interaction via hOAT1 and hOAT3, because there is a possibility that plasma concentrations of unbound MPA and MPAG will reach levels inhibitory to the transporters. Among drugs frequently administered to recipients of organ transplantations, ganciclovir and famotidine as well as acyclovir are substrates of hOAT1 or hOAT3 [16,17,32] and are myelosuppressive in addition to MPA. Furthermore, the present study shows that

MPAG is a substrate of hOAT3, suggesting that hOAT3 contributes to the renal tubular secretion of MPAG. These findings are useful for optimizing treatments for organ transplantation.

Acknowledgements

This work was supported in part by a grant-in-aid for Research on Advanced Medical Technology from the Ministry of Health, Labor and Welfare of Japan, by a Japan Health Science Foundation "Research on Health Sciences Focusing on Drug Innovation", by a grant-in-aid for Scientific Research from the Ministry of Education, Science, Culture and Sports of Japan and by the 21st Century COE program "Knowledge Information Infrastructure for Genome Science".

REFERENCES

[1] Bullingham R, Nicholls AJ, Kamm BR. Clinical pharmacokinetics of mycophenolate mofetil. Clin Pharmacokinet 1998;34:429–55.
[2] Picard N, Ratanasavanh D, Prémaud A, Le Meur Y, Marquet P. Identification of the UDP-glucuronosyltransferase isoforms involved in mycophenolic acid phase II metabolism. Drug Metab Dispos 2005;33:139–46.
[3] Bernard O, Guillemette C. The main role of UGT1A9 in the hepatic metabolism of mycophenolic acid and the effects of naturally occurring variants. Drug Metab Dispos 2004;32:775–8.
[4] Girard H, Court MH, Bernard O, Fortier LC, Villeneuve L, Hao Q, et al. Identification of common polymorphisms in the promoter of the UGT1A9 gene: evidence that UGT1A9 protein and activity levels are strongly genetically controlled in the liver. Pharmacogenetics 2004; 14:501–15.
[5] Gimenez F, Foeillet E, Bourdon O, Weller S, Garret C, Bidault R, et al. Evaluation of pharmacokinetic interactions after oral administration of mycophenolate mofetil and valaciclovir or aciclovir to healthy subjects. Clin Pharmacokinet 2004;43:685–92.
[6] Hesselink DA, van Hest RM, Mathot RA, Bonthuis F, Weimar W, de Bruin RW, et al. Cyclosporine interacts with mycophenolic acid by inhibiting the multidrug resistance-associated protein 2. Am J Transplant 2005;5:987–94.
[7] Cattaneo D, Perico N, Gaspari F, Gotti E, Remuzzi G. Glucocorticoids interfere with mycophenolate mofetil bioavailability in kidney transplantation. Kidney Int 2002;62:1060–7.
[8] Vietri M, Pietrabissa A, Mosca F, Pacifici GM. Mycophenolic acid glucuronidation and its inhibition by non-steroidal anti-inflammatory drugs in human liver and kidney. Eur J Clin Pharmacol 2000;56:659–64.
[9] Miyazaki H, Sekine T, Endou H. The multispecific organic anion transporter family: properties and pharmacological significance. Trends Pharmacol Sci 2004;25:654–62.
[10] Sweet DH. Organic anion transporter (Slc22a) family members as mediators of toxicity. Toxicol Appl Pharmacol 2005;204:198–215.
[11] Motohashi H, Sakurai Y, Saito H, Masuda S, Urakami Y, Goto M, et al. Gene expression levels and immunolocalization of organic ion transporters in the human kidney. J Am Soc Nephrol 2002;13:866–74.
[12] Uwai Y, Taniguchi R, Motohashi H, Saito H, Okuda M, Inui K. Methotrexate–loxoprofen interaction: involvement of human organic anion transporters hOAT1 and hOAT3. Drug Metab Pharmacokinet 2004;19:369–74.
[13] Ueo H, Motohashi H, Katsura T, Inui K. Human organic anion transporter hOAT3 is a potent transporter of cephalosporin antibiotics, in comparison with hOAT1. Biochem Pharmacol 2005;70:1104–13.
[14] Page 2nd RL, Miller GG, Lindenfeld J. Drug therapy in the heart transplant recipient—part IV: drug–drug interactions. Circulation 2005;111:230–9.
[15] Laskin OL. Clinical pharmacokinetics of acyclovir. Clin Pharmacokinet 1983;8:187–201.
[16] Takeda M, Khamdang S, Narikawa S, Kimura H, Kobayashi Y, Yamamoto T, et al. Human organic anion transporters and human organic cation transporters mediate renal antiviral transport. J Pharmacol Exp Ther 2002;300:918–24.
[17] Shitara Y, Horie T, Sugiyama Y. Transporters as a determinant of drug clearance and tissue distribution. Eur J Pharm Sci 2006;27:425–46.
[18] Bullingham R, Monroe S, Nicholls A, Hale M. Pharmacokinetics and bioavailability of mycophenolate mofetil in healthy subjects after single-dose oral and intravenous administration. J Clin Pharmacol 1996;36: 315–24.
[19] Nowak I, Shaw LM. Mycophenolic acid binding to human serum albumin: characterization and relation to pharmacodynamics. Clin Chem 1995;41:1011–7.
[20] Mudge DW, Atcheson BA, Taylor PJ, Pillans PI, Johnson DW. Severe toxicity associated with a markedly elevated mycophenolic acid free fraction in a renal transplant recipient. Ther Drug Monit 2004;26:453–5.
[21] Johnson HJ, Swan SK, Heim-Duthoy KL, Nicholls AJ, Tsina I, Tarnowski T. The pharmacokinetics of a single oral dose of mycophenolate mofetil in patients with varying degrees of renal function. Clin Pharmacol Ther 1998;63:512–8.
[22] Kaplan B, Meier-Kriesche H, Friedman G, Mulgaonkar S, Gruber S, Korecka M, et al. The effect of renal insufficiency on mycophenolic acid protein binding. J Clin Pharmacol 1999;39:715–20.
[23] Uwai Y, Okuda M, Takami K, Hashimoto Y, Inui K. Functional characterization of the rat multispecific organic anion transporter OAT1 mediating basolateral uptake of anionic drugs in the kidney. Fed Eur Biochem Soc Lett 1998;438:321–4.
[24] Uwai Y, Saito H, Hashimoto Y, Inui K. Inhibitory effect of anti-diabetic agents on rat organic anion transporter rOAT1. Eur J Pharmacol 2000;398:193–7.
[25] Mulato AS, Ho ES, Cihlar T. Nonsteroidal anti-inflammatory drugs efficiently reduce the transport and cytotoxicity of adefovir mediated by the human renal organic anion transporter 1. J Pharmacol Exp Ther 2000;295:10–5.
[26] Royer B, Zanetta G, Bérard M, Davani S, Tanter Y, Rifle G, et al. A neutropenia suggesting an interaction between valacyclovir and mycophenolate mofetil. Clin Transplant 2003;17:158–61.
[27] Sakurai Y, Motohashi H, Ueo H, Masuda S, Saito H, Okuda M, et al. Expression levels of renal organic anion transporters (OATs) and their correlation with anionic drug excretion in patients with renal diseases. Pharm Res 2004;21:61–7.
[28] Sakurai Y, Motohashi H, Ogasawara K, Terada T, Masuda S, Katsura T, et al. Pharmacokinetic significance of renal OAT3 (SLC22A8) for anionic drug elimination in patients with mesangial proliferative glomerulonephritis. Pharm Res 2005;22:2016–22.
[29] Alak AM. Measurement of tacrolimus (FK506) and its metabolites: a review of assay development and

application in therapeutic drug monitoring and pharmacokinetic studies. Ther Drug Monit 1997;19:338–51.
[30] Christians U, Sewing KF. Cyclosporin metabolism in transplant patients. Pharmacol Ther 1993;57:291–345.
[31] Chan GL, Erdmann GR, Gruber SA, Matas AJ, Canafax DM. Azathioprine metabolism: pharmacokinetics of 6-mercaptopurine, 6-thiouric acid and 6-thioguanine nucleotides in renal transplant patients. J Clin Pharmacol 1990;30:358–63.
[32] Motohashi H, Uwai Y, Hiramoto K, Okuda M, Inui K. Different transport properties between famotidine and cimetidine by human renal organic ion transporters (SLC22A). Eur J Pharmacol 2004;503:25–30.

BIOCHEMICAL PHARMACOLOGY 74 (2007) 359–371

available at www.sciencedirect.com

ScienceDirect

journal homepage: www.elsevier.com/locate/biochempharm

Substrate specificity of MATE1 and MATE2-K, human multidrug and toxin extrusions/H^+-organic cation antiporters

Yuko Tanihara [a], *Satohiro Masuda* [a], *Tomoko Sato* [a], *Toshiya Katsura* [a], *Osamu Ogawa* [b], *Ken-ichi Inui* [a,*]

[a] *Department of Pharmacy, Kyoto University Hospital, Sakyo-ku, Kyoto 606-8507, Japan*
[b] *Department of Urology, Graduate School of Medicine, Kyoto University, Sakyo-ku, Kyoto 606-8507, Japan*

ARTICLE INFO

Article history:
Received 21 February 2007
Accepted 6 April 2007

Keywords:
Brush-border membrane
Cephalexin
MATE1
MATE2-K
Organic cation

ABSTRACT

The substrate specificities of human (h) multidrug and toxin extrusion (MATE) 1 and hMATE2-K were examined to find functional differences between these two transporters by the transfection of the cDNA of hMATE1 and hMATE2-K into HEK293 cells. Western blotting revealed specific signals for hMATE1 and hMATE2-K consistent with a size of 50 and 40 kDa, respectively, in the transfectants as well as human renal brush-border membranes under reducing conditions. In the presence of oppositely directed H^+-gradient, the transport activities of various compounds such as tetraethylammonium, 1-methyl-4-phenylpyridinium, cimetidine, metformin, creatinine, guanidine, procainamide, and topotecan were stimulated in hMATE1- and hMATE2-K-expressing cells. In addition to cationic compounds, anionic estrone sulfate, acyclovir, and ganciclovir were also recognized as substrates of these transporters. Kinetic analyses demonstrated the Michaelis–Menten constants for the hMATE1-mediated transport of tetraethylammonium, 1-methyl-4-phenylpyridinium, cimetidine, metformin, guanidine, procainamide, topotecan, estrone sulfate, acycrovir, and ganciclovir to be (in mM) 0.38, 0.10, 0.17, 0.78, 2.10, 1.23, 0.07, 0.47, 2.64, and 5.12, respectively. Those for hMATE2-K were 0.76, 0.11, 0.12, 1.98, 4.20, 1.58, 0.06, 0.85, 4.32, and 4.28, respectively. Although their affinity for hMATE1 and hMATE2-K was similar, the zwitterionic cephalexin and cephradine were revealed to be specific substrates of hMATE1, but not of hMATE2-K. Levofloxacin and ciprofloxacin were not transported, but were demonstrated to be potent inhibitors of these transporters. These results suggest that hMATE1 and hMATE2-K function together as a detoxication system, by mediating the tubular secretion of intracellular ionic compounds across the brush-border membranes of the kidney.

1. Introduction

The oppositely directed H^+-gradient was demonstrated to be a driving force for the uptake of tetraethylammonium (TEA), a prototype substrate of the renal organic cation transport system, by rat renal brush-border membrane vesicles [1]. After that, various cationic drugs, toxins, and endogenous metabolites were revealed to be transported by the luminal H^+/

* *Corresponding author*. Tel.: +81 75 751 3577; fax: +81 75 751 4207.
E-mail address: inui@kuhp.kyoto-u.ac.jp (K. Inui).

Abbreviations: hOCT, human organic cation transporter; hMATE, human multidrug and toxin extrusion; MPP, 1-methyl-4-phenylpyridinium; TEA, tetraethylammonium

0006-2952/$ – see front matter © 2007 Elsevier Inc. All rights reserved.
doi:10.1016/j.bcp.2007.04.010

organic cation antiport system [2,3]. However, the molecular identification of the luminal H^+/organic cation antiport system had not been successful for more than 20 years.

A human (h) orthologue of the bacterial multidrug and toxin extrusion (MATE) family, hMATE1, was identified as a H^+-coupled organic cation exporter [4]. Recently, we have isolated a kidney-specific homologue, hMATE2-K [5]. Functional analyses using mammalian cells transfected with hMATE1 cDNA suggested that hMATE1 transported cationic compounds, TEA and 1-methyl-4-phenylpyridinium (MPP). It was also demonstrated that the hMATE1-mediated transport of TEA was inhibited by other compounds such as cimetidine [4]. We reported that rat (r) MATE1 transported not only cationic compounds but also zwitterionic or anionic compounds [6], and hMATE2-K transported various cationic compounds [5]. Although we reported that the anticancer drug oxaliplatin was preferentially transported by hMATE2-K [7,8], little is known about the physiological and pharmacological roles of hMATE1 and hMATE2-K, especially regarding the recognition of substrates.

In the present study, we have simultaneously demonstrated the substrate specificity of hMATE1 and hMATE2-K, by measuring the activity to transport for various ionic compounds, and found some substrates to be specific for hMATE1.

2. Materials and methods

2.1. Materials

[^{14}C]TEA (2.035 GBq/mmol), [^{14}C]creatinine (2.035 GBq/mmol), [^{14}C]procainamide (2.035 GBq/mmol), [methyl-^{14}C]-choline (2.035 GBq/mmol), [9-^{3}H]quinidine (740 GBq/mmol), [^{3}H]quinine (740 GBq/mmol), L-[*N*-methyl-^{3}H]carnitine (3.145 TBq/mmol), [*N*-methyl-^{14}C]nicotine (2.035 TBq/mmol), [*N*-methyl-^{3}H]verapamil (2.96 TBq/mmol), and [7-^{3}H (N)]tetracycline (185 GBq/mmol) were obtained from American Radiolabeled Chemicals Inc (St. Louis, MO). [^{14}C]Metformin (962 MBq/mmol), [^{14}C]guanidine hydrochloride (1.961 GBq/mmol), [^{3}H]ochratoxin A (666 GBq/mmol), [^{14}C]uric acid (1.961 GBq/mmol), [^{14}C]glysylsarcosine (4.07 GBq/mmol), [^{3}H]valproic acid (2.035 TBq/mmol), [^{3}H]acyclovir (407 GBq/mmol), [^{3}H]ganciclovir (370 GBq/mmol), [^{3}H]9-(2-phosphonylmethoxyethyl)-adenine (adefovir; 333 GBq/mmol), [^{3}H](S)-1-[3-hydroxy-2-(phosphonylmethoxy)propyl]-cytosine (cidofovir; 555 GBq/mmol), and [^{3}H]9-(2-phosphonylmethoxypropyl)-adenine (tenofovir; 370 GBq/mmol) were purchased from Moravek Biochemicals Inc. (Brea, CA). [^{3}H]MPP (2.7 TBq/mmol), [^{14}C]para-aminohippuric acid (1.9 GBq/mmol), [^{3}H]dehydroepiandrosterone sulfate (2.22 TBq/mmol), [^{14}C]salicylic acid (1.7 GBq/mmol), [^{14}C]indomethacin (740 MBq/mmol), [^{3}H]prostaglandin F_2 alpha (6.66 TBq/mmol), and [^{3}H]estrone sulfate (2.12 TBq/mmol) were from PerkinElmer Life Analytical Sciences (Boston, MA). [N-Methyl-^{3}H]Cimetidine (451 GBq/mmol) was from Amersham Biosciences (Uppsala, Sweden). Acyclovir was obtained from Sigma (St. Louis, MO). [^{14}C]Levofloxacin (1.07 GBq/mmol, Daiichi Pharmaceutical Co., Tokyo, Japan), [^{14}C]captopril (0.115 GBq/mmol, Sankyo Co., Tokyo, Japan), cephalexin (Shionogi, Osaka, Japan), cefazolin (Astellas Pharma Inc., Tokyo, Japan), cephradine (Sankyo Co., Tokyo, Japan), ciprofloxacin hydrochloride (Bayer AG, Leverkusen, Germany), [^{14}C]SK&F 104864 (topotecan; 1.78 GBq/mmol, Nippon Kayaku Co., Tokyo, Japan), and unlabeled SK&F 104864 (topotecan; Nippon Kayaku Co., Tokyo, Japan) were kindly provided by the respective suppliers. All other chemicals used were of the highest purity available.

2.2. Cell culture and transfection

HEK293 cells (American Type Culture Collection CRL-1573, Manassas, VA) were cultured in complete medium consisting of Dulbecco's modified Eagle's medium (Sigma Chemical Co., St. Louis, MO) with 10% fetal bovine serum (Invitrogen, Carlsbad, CA) in an atmosphere of 5% CO_2/95% air at 37 °C, and used as host cells. hMATE1 and hMATE2-K cDNAs were subcloned into the pcDNA3.1/Hygro (+) plasmid vector (Invitrogen) as previously described [7]. HEK293 cells were transfected with hMATE1 cDNA, hMATE2-K cDNA, or pcDNA3.1 (+) empty vector using LipofectAMINE 2000 Reagent (Invitrogen) according to the manufacturer's instructions. At 48 h after transfection, the cells were used for uptake experiments. To construct transfectants stably expressing hMATE1 or hMATE2-K, hygromycin B (0.2 mg/mL, Invitrogen) -resistant single colonies were picked out. Cells expressing hMATE1 (HEK-hMATE1) or hMATE2-K (HEK-hMATE2-K) were selected by measuring [^{14}C]TEA uptake. The stable transfectant of pcDNA3.1 (+) empty vector (HEK-VECTOR) was established as previously described [9]. The cell monolayers at day 3 of culture were used for uptake experiments.

2.3. Antibodies and Western blot analysis

Rabbit anti-hMATE1 and hMATE2-K antibodies were prepared as described previously [5]. For the Western blot analysis, crude plasma membranes (20 μg) were obtained from HEK293 cells stably transfected with vector alone (pcDNA3.1 (+)), hMATE1, and hMATE2-K, and were prepared as described previously with some modifications [9]. The brush-border membrane fractions were obtained from human renal cortex as described previously [10,11]. The membrane fractions were suspended in buffer (100 mM mannitol and 10 mM HEPES-KOH, pH 7.5) and solubilized in NuPAGE® LDS sample buffer (Invitrogen) with or without 50 mM dithiothreitol and heated at 70 °C for 10 min. The samples were separated by SDS-polyacrylamide gel electrophoresis (4–12% NuPAGE® Novex Bis–Tris Gel; Invitrogen) and transferred to polyvinylidene difluoride membranes (PVDF membrane 0.2 μm; Invitrogen) using an XCell II® Blot Module (Invitrogen) according to the manufacturer's instructions. The blots were incubated with antisera specific for hMATE1 (1:1000 dilution) and hMATE2-K (1:2000), respectively. The bound antibody was detected on X-ray film by enhanced chemiluminescence with horseradish peroxidase-conjugated anti-rabbit IgG antibody and cyclic diacylhydrazides (GE Healthcare Bio-Science Corp., Piscataway, NJ). To confirm the specificity of polyclonal antibodies, each antibody was absorbed with an excess amount of antigen peptide (20 μg/mL) used as an immunogen and processed similarly.

2.4. Uptake experiments

Cellular uptake of ionic compounds was measured with cultures of HEK293 cells grown on poly-D-lysine-coated 24-well plates [9,12]. Typically, the cells were preincubated with 0.2 mL of incubation medium (145 mM NaCl, 3 mM KCl, 1 mM $CaCl_2$, 0.5 mM $MgCl_2$, 5 mM D-Glucose, and 5 mM HEPES, pH 7.4) for 10 min at 37 °C. The medium was then removed, and 0.2 mL of incubation medium containing radiolabeled substrates was added. The medium was aspirated off after the defined time for incubation, and the monolayers were rapidly rinsed three times with 1 mL of ice-cold incubation medium. The cells were solubilized in 0.5 mL of 0.5N NaOH, and then the radioactivity in aliquots was measured by liquid scintillation counting. The cellular uptake of cephalexin, cephradine, and cefazolin was performed as described previously [5,13]. To manipulate the intracellular pH, intracellular acidification was performed by pretreatment in the incubation medium with ammonium chloride (30 mM, 20 min at 37 °C, pH 7.4) [14,15]. When extracellular pH was varied between 6.0 and 9.0, buffering agents were MES (2-(N-morpholino)ethanesulfonic acid) for pH 6.0, 6.5 and 7.0, and HEPES for pH 7.5, 8.0, 8.5 and 9.0. The protein concentration of the solubilized cells was determined using a Bio-Rad Protein Assay Kit (Bio-Rad Laboratories, Hercules, CA) with bovine gamma-globulin as a standard.

2.5. Statistical analysis

Data are expressed as the mean ± S.E. Data were analyzed statistically using an unpaired t test. Significance was set at $P < 0.05$. In all figures, when error bars are not shown, they are smaller than the symbols.

3. Results

3.1. Substrate screening of hMATE1 and hMATE2-K

The uptake of various organic ions was examined in HEK293 cells transiently transfected with the pcDNA3.1 (+) empty vector, hMATE1 cDNA, and hMATE2-K cDNA, respectively. The uptake experiment at the extracellular pH 8.4 showed the good substrates of rMATE1 and hMATE2-K, and the relatively weak substrates for both transporters were confirmed by the uptake experiment after pretreatment of ammonium chloride generating the intracellular acidification [5,6]. Therefore, we employed these two conditions to demonstrate the substrate specificities of hMATE1 and hMATE2-K. The transfection of hMATE1 or hMATE2-K cDNA stimulated the oppositely-directed H^+-gradient-dependent transport of structurally diverse organic cations such as [^{14}C]TEA, [^{3}H]MPP, [^{3}H]cimetidine, [^{14}C]metformin, [^{14}C]creatinine, [^{14}C]guanidine, [^{14}C]procainamide, and [^{14}C]topotecan at the extracellular pH 8.4 (Table 1). The intracellular acidification resulted in marked stimulation of uptake compared to the change of extracellular pH (Table 2). The uptake of an anionic compound, [^{3}H]estrone sulfate, was also enhanced in the cells transfected with the hMATE1- or hMATE2-K-cDNA in both conditions. The uptake of [^{3}H]acyclovir was markedly increased in the hMATE1- and hMATE2-K-expressing cells after the pretreatment with ammonium chloride (Tables 1 and 2). The uptake of

Table 1 – Uptake of various organic ions in HEK293 cells expressing hMATE1 and hMATE2-K at extracellular pH 8.4

Compounds	Concentration (μM)	Uptake (μl/mg protein/15 min)		
		Vector	hMATE1	hMATE2-K
[^{14}C]TEA	5.0	0.33 ± 0.09	40.8 ± 3.00*** 123†	10.1 ± 0.67*** 31†
[^{3}H]MPP	0.004	11.0 ± 0.59	96.3 ± 4.96*** 8.7	22.5 ± 1.51** 2.0
[^{3}H]cimetidine	0.023	1.13 ± 0.10	6.97 ± 0.60*** 6.2	2.87 ± 0.20** 2.5
[^{14}C]metformin	9.9	0.82 ± 0.09	63.7 ± 1.22*** 78	9.48 ± 0.23*** 12
[^{14}C]creatinine	5.0	1.33 ± 0.04	2.93 ± 0.27** 2.2	1.75 ± 0.14* 1.3
[^{14}C]guanidine	5.3	9.02 ± 0.53	14.9 ± 0.95** 1.7	6.85 ± 0.27* 0.8
[^{14}C]procainamide	5.0	13.2 ± 0.57	47.6 ± 3.20*** 3.6	26.5 ± 1.53** 2.0
[^{14}C]choline	5.0	40.3 ± 2.79	46.3 ± 2.12 1.2	43.2 ± 0.90 1.1
[^{3}H]quinidine	0.014	309 ± 8.06	305 ± 32.9 1.0	320 ± 7.29 1.0
[^{3}H]quinine	0.014	160 ± 5.78	187 ± 2.23* 1.2	199 ± 15.1 1.2
[^{3}H]thiamine	0.028	13.4 ± 0.47	27.8 ± 0.85*** 2.1	18.1 ± 0.96* 1.4

Table 1 (*Continued*)

Compounds	Concentration (μM)	Uptake (μl/mg protein/15 min)		
		Vector	hMATE1	hMATE2-K
[^{3}H]carnitine	0.003	44.5 ± 2.98	36.4 ± 2.29 0.8	29.3 ± 1.82* 0.7
[^{14}C]nicotine	5.0	5.51 ± 0.54	7.65 ± 1.04 1.4	7.77 ± 0.30* 1.4
[^{14}C]captopril	90	0.32 ± 0.07	0.54 ± 0.04 1.7	0.33 ± 0.07 1.0
[^{3}H]verapamil	0.004	49.9 ± 4.10	42.8 ± 0.54 0.9	60.1 ± 7.35 1.2
[^{14}C]levofloxacin	14	4.01 ± 0.20	4.95 ± 0.14* 1.2	3.98 ± 0.07 1.0
[^{3}H]tetracycline	0.056	7.03 ± 0.36	6.32 ± 0.93 0.9	8.86 ± 0.24* 1.3
[^{14}C]topotecan	5.8	6.33 ± 0.27	9.30 ± 0.13*** 1.5	6.73 ± 0.32* 1.1
[^{14}C]para-aminohippuric acid	5.6	4.68 ± 0.53	4.06 ± 0.07 0.9	3.13 ± 0.05* 0.7
[^{3}H]estrone sulfate	0.005	1.91 ± 0.11	3.85 ± 0.17*** 2.0	4.22 ± 0.16*** 2.2
[^{3}H]ochratoxin A	0.016	3.96 ± 0.55	2.80 ± 0.23 0.7	3.66 ± 0.29 0.9
[^{3}H]dehydroepiandrosterone sulfate	0.005	19.9 ± 1.73	19.8 ± 1.08 1.0	20.4 ± 1.26 1.0
[^{14}C]uric acid	5.3	0.75 ± 0.04	1.04 ± 0.26 1.4	1.06 ± 0.16 1.4
[^{14}C]salicylic acid	5.8	1.62 ± 0.16	2.20 ± 0.09* 1.4	2.00 ± 0.34 1.2
[^{14}C]indomethacin	13	9.96 ± 0.60	9.23 ± 0.60 0.9	12.4 ± 1.25 1.3
[^{3}H]prostaglandin F_2 alpha	0.002	1.45 ± 0.19	1.03 ± 0.08 0.7	2.04 ± 0.19 1.4
[^{3}H]valproic acid	0.006	0.50 ± 0.01	0.54 ± 0.04 1.1	0.57 ± 0.01 1.1
[^{3}H]acyclovir	0.092	1.74 ± 0.16	2.54 ± 0.26 1.5	1.53 ± 0.74 0.9
[^{3}H]ganciclovir	0.028	1.40 ± 0.12	1.48 ± 0.37 1.1	2.44 ± 0.18** 1.7
[^{3}H]adefovir	0.031	1.30 ± 0.09	1.07 ± 0.10 0.8	1.40 ± 0.08 1.1
[^{3}H]cidofovir	0.017	0.28 ± 0.04	0.34 ± 0.03 1.2	0.20 ± 0.03 0.7
[^{3}H]tenofovir	0.028	0.85 ± 0.11	1.26 ± 0.10* 1.5	1.10 ± 0.09 1.3
[^{14}C]glycylsarcosine	2.5	0.27 ± 0.06	0.23 ± 0.02 0.9	0.21 ± 0.02 0.8

HEK293 cells cultured in a 24-well plate were transfected with the empty vector (Vector), hMATE1 cDNA, or hMATE2-K cDNA, and incubated for 15 min at pH 8.4 in medium containing the 33 radiolabeled compounds indicated. The radioactivity of solubilized cells was then determined. Uptake was expressed as clearance, which was obtained by dividing the net uptake value by each concentration of substrate in the medium. Data represent the mean ± S.E. for three monolayers from a typical experiment in at least three separate experiments. †Below each uptake value is the uptake ratio compared to vector-transfected cells.

* $P < 0.05$ significantly different from vector-transfected cells.

** $P < 0.01$ significantly different from vector-transfected cells.

*** $P < 0.001$ significantly different from vector-transfected cells.

Table 2 – Uptake of various organic ions in HEK293 cells expressing hMATE1 and hMATE2-K at extracellular pH 7.4 after pretreatment with ammonium chloride

Compounds	Concentration (μM)	Uptake (μl/mg protein/2 min)		
		Vector	hMATE1	hMATE2-K
[^{14}C]TEA	5.0	0.28 ± 0.02	20.7 ± 1.56*** 74†	6.47 ± 0.17*** 23†
[^{3}H]MPP	0.004	2.92 ± 0.35	51.0 ± 4.29*** 17	16.4 ± 0.95*** 5.6
[^{3}H]cimetidine	0.023	2.62 ± 0.22	30.3 ± 2.47*** 12	12.5 ± 0.57*** 4.8
[^{14}C]metformin	9.9	0.35 ± 0.04	29.0 ± 1.23*** 83	4.20 ± 0.12*** 12
[^{14}C]creatinine	5.0	0.41 ± 0.04	2.76 ± 0.11*** 6.7	0.69 ± 0.05* 1.7
[^{14}C]guanidine	5.3	2.60 ± 0.08	4.09 ± 0.16** 1.6	3.05 ± 0.03** 1.2
[^{14}C]procainamide	5.0	13.2 ± 0.77	23.7 ± 0.49*** 1.8	16.0 ± 0.61* 1.2
[^{14}C]choline	5.0	6.81 ± 0.18	7.55 ± 0.37 1.1	6.61 ± 0.38 1.0
[^{3}H]quinidine	0.014	87.6 ± 7.05	103 ± 5.12 1.2	84.3 ± 4.45 1.0
[^{3}H]quinine	0.014	65.9 ± 4.36	91.1 ± 4.81* 1.4	80.3 ± 7.02 1.2
[^{3}H]thiamine	0.028	3.73 ± 0.30	10.2 ± 0.30*** 2.8	5.67 ± 0.13** 1.5
[^{3}H]carnitine	0.003	8.98 ± 0.31	8.31 ± 0.37 0.9	8.56 ± 0.16 1.0
[^{14}C]nicotine	5.0	2.62 ± 0.34	3.12 ± 0.16 1.2	2.91 ± 0.16 1.1
[^{14}C]captopril	90	0.13 ± 0.04	0.31 ± 0.08 2.4	0.27 ± 0.09 2.1
[^{3}H]verapamil	0.004	29.3 ± 1.44	25.0 ± 0.92 0.9	31.3 ± 2.31 0.9
[^{14}C]levofloxacin	14	5.95 ± 0.11	7.31 ± 0.32* 1.2	5.90 ± 0.20 1.0
[^{3}H]tetracycline	0.056	2.37 ± 0.23	2.72 ± 0.24 1.2	2.49 ± 0.21 1.1
[^{14}C]topotecan	5.8	6.04 ± 0.20	8.71 ± 0.42** 1.4	8.78 ± 0.50** 1.5
[^{14}C]para-aminohippuric acid	5.6	1.01 ± 0.02	1.11 ± 0.26 1.1	1.15 ± 0.06 1.1
[^{3}H]estrone sulfate	0.005	1.23 ± 0.04	4.49 ± 0.43** 3.7	2.40 ± 0.16** 2.0
[^{3}H]ochratoxin A	0.016	4.08 ± 0.74	3.33 ± 0.34 0.8	2.45 ± 0.02 0.6
[^{3}H]dehydroepiandrosterone sulfate	0.005	10.3 ± 0.48	10.6 ± 0.61 1.0	10.7 ± 0.14 1.0
[^{14}C]uric acid	5.3	0.35 ± 0.05	0.36 ± 0.01 1.0	0.39 ± 0.01 1.1
[^{14}C]salicylic acid	5.8	0.49 ± 0.05	0.65 ± 0.08 1.3	0.45 ± 0.08 0.9
[^{14}C]indomethacin	13	5.04 ± 0.28	4.52 ± 0.21 0.9	5.61 ± 0.22 1.1

Table 2 (*Continued*)

Compounds	Concentration (μM)	Uptake (μl/mg protein/2 min)		
		Vector	hMATE1	hMATE2-K
[^{3}H]prostaglandin F_2 alpha	0.002	0.59 ± 0.11	0.77 ± 0.06 1.3	0.93 ± 0.02 1.6
[^{3}H]valproic acid	0.006	0.19 ± 0.09	0.14 ± 0.08 0.7	0.29 ± 0.13 1.5
[^{3}H]acyclovir	0.092	0.43 ± 0.05	1.28 ± 0.13** 3.0	1.03 ± 0.13* 2.4
[^{3}H]ganciclovir	0.028	0.41 ± 0.03	0.74 ± 0.07* 1.8	1.60 ± 0.12*** 3.9
[^{3}H]adefovir	0.031	0.29 ± 0.03	0.26 ± 0.08 0.9	0.29 ± 0.03 1.0
[^{3}H]cidofovir	0.017	0.09 ± 0.03	0.10 ± 0.03 1.1	0.09 ± 0.03 1.0
[^{3}H]tenofovir	0.028	0.18 ± 0.05	0.20 ± 0.04 1.1	0.17 ± 0.05 0.9
[^{14}C]glycylsarcosine	2.5	0.12 ± 0.03	0.12 ± 0.06 1.0	0.12 ± 0.02 1.0

HEK293 cells cultured in a 24-well plate to examine the uptake of radiolabeled compounds were transfected with the empty vector (Vector), hMATE1 cDNA or hMATE2-K cDNA, and incubated for 20 min with medium containing 30 mM ammonium chloride. After washing, 2 min uptake measurements at extracellular pH 7.4 were carried out as described in the legend for Table 1. Data represent the mean ± S.E. for three monolayers from a typical experiment in at least three separate experiments. †Below each uptake value is the uptake ratio compared to vector-transfected cells.

* $P < 0.05$ significantly different from vector-transfected cells.

** $P < 0.01$ significantly different from vector-transfected cells.

*** $P < 0.001$ significantly different from vector-transfected cells.

[^{3}H]ganciclovir was stimulated in the hMATE2-K-expressing cells but not in the hMATE1-expressing cells at the extracellular pH 8.4, and it was also stimulated in the hMATE1-expressing cells after pretreatment with ammonium chloride (Tables 1 and 2).

3.2. *Construction of HEK293 cells stably expressing hMATE1 and hMATE2-K*

To obtain quantitative information about the hMATE1- or hMATE2-K-mediated transport of ionic compounds, we constructed HEK 293 cells stably expressing hMATE1 (HEK-hMATE1) and hMATE2-K (HEK-hMATE2-K). The protein expression of hMATE1 in HEK-hMATE1 cells and hMATE2-K in HEK-hMATE2-K cells was confirmed by Western blotting with specific antibody for each transporter. In the nonreducing and reducing conditions, immunoreactive protein was detected in each stable transfectant with an apparent molecular mass of 50 kDa for anti-hMATE1 antibody (Fig. 1A and C), and 40 kDa for anti-hMATE2-K antibody (Fig. 1E and G), respectively. No signal was observed in another transfectant or the vector-transfected control. These positive bands disappeared when the antiserum was preabsorbed with each antigen peptide (Fig. 1B, D, F and H). Consistent with the protein expression in each transfectant, specific signals for hMATE1 (Fig. 1A and C) and hMATE2-K (Fig. 1E and G) were observed in the human renal brush-border membranes, both of which were abolished with the antigen-preabsorbed antibodies (Fig. 1B, D, F and H). The functional expression of hMATE1 and hMATE2-K was assessed by the uptake of [^{14}C]TEA by HEK-hMATE1 and HEK-hMATE2-K cells, respectively. Both the hMATE1- and hMATE2-K-mediated uptake of [^{14}C]TEA without pretreatment with ammonium chloride increased in accordance with the extracellular pH between 6.0 and 9.0 (Fig. 2A), and increased in a time-dependent manner (Fig. 2B). After the pretreatment with ammonium chloride, the uptake of [^{14}C]TEA in the HEK-hMATE1 and HEK-hMATE2-K cells also increased with extracellular pH between 6.0 and 9.0. The uptake was greatest and lowest at an extracellular pH of 8.5 and 6.0, respectively (Fig. 2C). Although the apparent linearity of the time course of the hMATE1- and hMATE2-K-mediated uptake of [^{14}C]TEA was less than 30 s in the condition of the cellular acidification (Fig. 2D), the transport characteristics of hMATE1 and hMATE2-K in the transfectants pretreated with ammonium chloride were examined at 2 min in subsequent experiments for reasons of technical limitations and reproducibility.

3.3. *Comparison of functional characteristics between hMATE1 and hMATE2-K*

The uptake of TEA, MPP, cimetidine, metformin, guanidine, procainamide, topotecan, estrone sulfate, acycrovir, and ganciclovir at extracellular pH 7.4 after pretreatment with ammonium chloride by hMATE1 and hMATE2-K exhibited saturable kinetics, following the Michaelis-Menten equation. The apparent K_m and maximal uptake velocity (V_{max}) values of TEA, MPP, cimetidine, metformin, guanidine, procainamide, topotecan, estrone sulfate, acycrovir, and ganciclovir are shown in Table 3. The K_m values for hMATE1-mediated